Republic of Iraq
Ministry of Higher Education and Scientific Research
University of Babylon
College of medicine
Department of Medical Physiology

Evaluation of Left Ventricular Remodelling in Anterior Myocardial Infarction Patients by 2 and 3 D-Echocardiographic Derived Sphericity Index and ECG

A Thesis

Submitted to the Council of College of Medicine, University of Babylon in Partial Fulfillment of the Requirements for the Degree of Master of Science/ Medical Physiology

By

Fatima Adnan Shaheed Jaber

M.B.Ch.B., College of Medicine/Babylon university

Supervised By

Asst. prof.

Dr. Ahlam Kadhim Abbood

PhD (Medical Physiology)
University of Babylon

Asst. Prof.

Dr. Shokry Faaz Nassir

F.I.B.M.S (Cardiol)
University of Babylon

2023 A.D **1444 A.H**

بِسْمِ اللَّهِ الرَّحْمَٰنِ الرَّحِيم

فَتَعَالَى اللَّهُ الْمَلِكُ الْحَقُّ ۗ وَلَا تَعْجَلْ بِالْقُرْآنِ مِن قَبْلِ أَن

يُقْضَىٰ إِلَيْكَ وَحْيُهُ ۖ وَقُل رَّبِّ زِدْنِي عِلْمًا ﴿١١٤﴾

صدق الله العلي العظيم

سورة طه آيه (١١٤)

Supervisor Certificate

I certify that this thesis entitled **"Evaluation of Left Ventricular Remodelling in Anterior Myocardial Infarction Patients by 2 and 3 D-Echocardiographic Derived Sphericity Index and ECG "** was carried out under my supervision at College of Medicine / University of Babylon, as a partial fulfillment of the requirements for the degree of ***"Master of Science in Medical Physiology".***

Signature

Asst. Prof. Dr. Ahlam Kadhim Abbood

College of Medicine/ University of Babylon

Signature

Asst. Prof. Dr. Shokry Faaz Nassir

College of Medicine/ University of Babylon

In view of the available recommendations, I forward this thesis for debate by the examining committee.

Signature

Prof. Dr. Samir Sawadi Al-jubori

Chairman of Medical Physiology Department

College of Medicine / University of Babylon

Examining Committee Certification

We, the examining committee, certify that we had read this thesis entitled "**Evaluation of Left Ventricular Remodelling in Anterior Myocardial Infarction Patients by 2 and 3 D-Echocardiographic Derived Sphericity Index and ECG**" and had examined the student "**Fatima A. Shaheed**" in its contents, and that, in our opinion, it is accepted as a thesis for the degree of Master of Sciences in Medical Physiology with "**Excellent**" estimation.

Prof. Dr. Amina Abdul Baqi Khuther
College of Medicine-University of Kufa
(Chairman)

Prof. Dr. Hassan Salim Al-Jumaily
College of Medicine-University of Babylon
(Member)

Asst. Prof. Dr. Zainab Falah Hassan
College of Medicine-University of Babylon
(Member)

Asst. Prof. Dr. Ahlam Kadhim Abbood
College of Medicine/ University of Babylon
(Member and supervisor)

Asst. Prof. Dr. Shokry Faaz Nassir
College of Medicine/ University of Babylon
(Member and supervisor)

Approved for the college committee of postgraduate studies

Prof. Dr. Mohend Abbass Alshalah
Dean of College

Dedication

To my mother's pure soul who taught me to trust God, to believe in hard work and that much can be done with a little.

To my father, who was the first educator, thank you for your support and encouragement.

To my family, for everything you have done for me.

Fatima Adnan

ACKNOWLEDGMENT

I would like to thank my God Almighty who is always there when I am in need. Thank you for guiding me and giving me strength in my daily life.

Also, I want to express my sincere thanks to my supervisor, Asst. Prof. Dr. Ahlam Kadhim Abbood for her guidance, support, and patience for all the fatigue and effort she endured in order to complete this study.

My thanks also extend to Asst. Prof. Dr. Shokry Faaz Nassir for his efforts in this study.

Also, my gratitude goes to the doctors of Shaheed Almehrab cardiac catheterization Center, Dr. Bassim Mohammed, Dr. Alaa Yousif, Dr. Wissam Saaed for their cooperation.

Also, my gratitude goes to the staff of echocardiography unit at Merjan Medical City, and the students of the Echo Diploma for their help and cooperation.

To express my thanks to all participant who contributed to the success of this study.

Fatima Adnan

Summary

Anterior myocardial infarction (MI) carries the poorest prognosis of all infarct locations, due to the larger area of myocardium infarct size, it leads to a sequence of structural changes that alter the size and shape of the left ventricle. The heart undergoes extensive myocardial remodelling through the accumulation of fibrous tissue in both the infarcted and non-infarcted myocardium, which distorts tissue structure, increases tissue stiffness, and causes ventricular dysfunction. The sphericity index (SI) has been used to measure global left ventricular (LV) shape, but it fails to detect regional shape abnormalities that occur at the apical area, so a straightforward measurement termed the conicity index (CI) was identified to measure these changes. An electrocardiographic (ECG) technique called the Selvester QRS Score was created for estimating infarct size following MI, it has the benefit of being both affordable and accessible.

This study aims to evaluate the role of the LV sphericity index in quantification of left ventricle geometric changes and studying its relationship to the systolic and diastolic work of the heart, beside role of the conicity index in reflecting the regional changes in the LV geometry, and also examine the role of the Selvester QRS score in determining the extent of myocardial scar in patients with anterior MI and its relation with LV remodelling.

This case-control study was conducted on 100 subjects (50 patients diagnosed with an old anterior myocardial infarction and 50 healthy subjects).

The study was conducted in Shaheed Almehrab cardiac catheterization center and Merjan Medical City in Al-Hilla City, Babylon Governorate,

through the period from start of September 2022 until start of February 2023.

The participants underwent echocardiographic (echo) with two and three dimensional (2D and 3D) modalities, by 2D echo, the long and the short axes of the left ventricle were measured and their ratio calculated as SI, also the apical axis length of the LV was measured and the ratio between the apical and short axis length was calculated as CI. The sphericity index was also measured by 3D echo and mathmatically by volume ratio (SIv), as the ratio between the LV end diastolic volume (EDV) to the hypothetical sphere volume ($1/6*\pi*L^3$, where L is the long axis of the LV). Correlations between these indices and the systolic and diastolic functions of the left ventricle were studied. The QRS score was calculated from the ECG, and the correlation between infarct size and LV remodelling parameters was checked.

Statistically significant differences were present between the patient and control groups regarding the values of 2D-SI, 3D-SI, SIv, and CI ($p < 0.05$).

The 2D,3D sphericity index showed a high statistically significant negative correlation with 2D,3D-ejection fraction (EF), ($P< 0.000$), and a statistically significant negative correlation with stroke volume (SV) ($p<0.05$).

The Conicity index Showed a statistically non-significant negative correlation with 2D, 3D derived EF and SV ($P > 0.05$)

Regarding the correlation studies of CI and SI with LV diastolic parameters (E/A, E/e' and tricuspid regurgitation (TR) velocity) showed positive correlation but statistically non-significant ($p > 0.05$) and

significant positive correlation of 2D,3D-SI with left atrial volume index (LAVI) ($p < 0.05$).

Correlation studies of LV infarct size by selvestor score with LV remodelling indices (2D, 3D-SI, CI) showed positive correlation but statistically non-significant with 2D-SI and statistically significant correlation with 3D-SI (P=0.377, 0.044 ,respectively), no significant correlation with CI ($p > 0.05$).

We conclude that echocardiographically determined LV indices are a straightforward noninvasive measure of LV remodelling either regionally by CI or globally by 2,3D-SI and from the correlation studies can reflect the systolic and diastolic function of the LV, and also the Selvester QRS score was feasible for detecting myocardial scarring in patients with anterior MI and can reflects the left ventricular remodelling through its relationship with 2D and 3D-SI, but cannot reflect the regional changes represented by CI.

List of abbreviation

Abbreviation	Meaning
AMI	Acute myocardial infarction
AUC	Area under the curve
AV	Atrioventricular
BMI	Body mass index
BSA	Body surface area
Cc	Cubic centimeter
CI	Conicity index
Cm	Centimeter
CMR	Cardiac magnetic resonance
DD	Diastolic dysfunction
2DE	Two dimensional echocardiography
3DE	Three dimensional echocardiography
2D-EDV	Two dimensional end diastolic volume
3D-EDV	Three dimensional end diastolic volume
2D-ESV	Two dimensional end systolic volume
3D-ESV	Three dimensional end systolic volume
2D-EF	Two dimensional ejection fraction
3D-EF	Three dimensional ejection fraction
2D-SI	Two dimensional sphericity index
3D-SI	Three dimensional sphericity index
2D-SV	Two dimensional stroke volume
3D-SV	Three dimensional stroke volume
ECG	Electrocardiogram
Echo	Echocardiographic
EDV	End diastolic volume

EF	Ejection fraction
ESV	End systolic volume
HDL	High-density lipoprotein
HF	Heart failure
ICD	Implantable cardioverter defibrillator
IHD	Ischemic heart disease
Kg	Kilogram
LA	Left atrium
LAD	Left anterior descending
LAFB	Left anterior fascicular block
LAVI	Left atrial volume index
LBBB	Left bundle branch block
LDL	Low density lipoproteins
LV	Left ventricle
LVDD	left ventricular diastolic dysfunction
LVEDV	Left ventricular end diastolic volume
LVEF	Left ventricular ejection fraction
LVESV	Left ventricular end systolic volume
LVH	Left ventricular hypertrophy
m^2	Square meter
MI	Myocardial infarction
MR	Mitral regurgitation
MRI	Magnetic resonance imaging
MV	Mitral valve
P	Probability
PCI	Percutaneous coronary intervention
RAAS	Renin angiotensin aldosterone system
RBBB	Right bundle branch block

ROC	Receiver operating characteristic
ROA	Right atrial overload
RWT	Relative wall thickness
S	Second
SA	Sinoatrial
SD	Standard deviation
SI	Sphericity index
SPI	Sphericity index
SIv	Sphericity index by equation
SNS	Sympathetic nervous system
STEMI	ST-segment elevation myocardial infarction
SV	Stroke volume
TR	Tricuspid regurgitation
VC	Vena contracta

List of content

List of tables

List of figures

CHAPTER ONE

INTRODUCTION

CHAPTER ONE

INTRODUCTION

1.1. Introduction:

Ischemic heart disease (IHD) is defined as a reduction in the blood flow to the heart muscle owing to the occlusion of the coronary artery by intravascular plaque that has gathered over time or embolization with a thrombus (Nowbar *et al*., 2019). IHD is the first ranked and most prevalent among cardiovascular diseases (Roth *et al*., 2017). Despite the mortality rate from ischemic heart disease having declined in the last four decades in developed countries, it remains to cause about one third of all deaths in people older than 35 years (Aggarwal *et al*., 2016).

Myocardial infarction is the most common form of IHD, MI is a continued hypoxia and ischemia of the myocardium as a consequence of acute occlusion of the coronary artery that causes myocardial necrosis (Thygesen *et al*., 2018). The most important risk factors of MI are hypertension, diabetes mellitus, obesity, alcohol consumption, dyslipidemia, smoking, and physical inactivity (Rathore *et al*., 2018).

The left anterior descending (LAD) coronary artery supplies the anterior myocardium, persistent ischemia due to LAD artery obstruction causes anterior MI, this process characteristically affects the anterior and apical walls of the left ventricle (Ghadri *et al*., 2018). Anterior myocardial infarction carries the poorest prognosis of all infarct locations, due to the larger area of myocardium infarct size (Ferrante *et al*., 2021).

In about 30% of patients with a previous anterior MI and 17% of patients with non-anterior infarct, post infarct ventricular remodelling occurs (Masci *et al*., 2011). Ventricular remodelling is a collection of molecular, cellular, and interstitial changes which appear as changes in the volume, function, and geometry of the heart after damage (Azevedo *et al*., 2015). The mechanisms that lead to LV remodelling post MI include infarct expansion, infarct extension into adjacent non infarcted myocardium, and hypertrophy in the remote LV (Elden, 2015).

The regulatory pathway for the development of adverse cardiac remodelling is a neurohormone, the main cardioregulatory hormonal cascades involved in left ventricle (LV) remodelling comprise the sympathetic nervous system (SNS) and the renin angiotensin aldosterone system (RAAS) (Bhatt *et al*., 2017).

Post infarct ventricular remodelling means an increase in the left ventricular chamber, which passes from an elliptical to a more spherical form. This alteration is expressed by an increase in the sphericity index (SI). Several geometrical indexes have been suggested to assess this deformation, such as the sphericity and conicity indexes (CI) (Pezel *et al*., 2020).

Left ventricular sphericity index is a rapid, simple, and reproducible measure to assess LV geometric changes, it was computed as the ratio between the short and long axis length. Left ventricle SI is reflective of geometric changes in the left ventricle and is related to adverse cardiovascular events in patients with anterior MI (Khanna *et al*., 2020).

Since SI cannot identify the local shape abnormalities at the apical region after anterior MI, which precede global ventricular dilatation, the conicity index is provided as a simple measure to address this focal change. CI is remarkably higher in anterior ischemic patients compared to normal people because this index measures the changes in an enlarged, less conical apex (Di Donato *et al*., 2006).

The LV apex was mainly involved after an anterior MI, so the local changes affected the anterior and septal ventricular constituents, as a result, the conicity index was noticeably greater in anterior remodelling (Garatti *et al*., 2015).

1.2. Aims of study:

This study aims to evaluate:

1. The role of the LV sphericity index in the quantification of left ventricle geometric changes and study its relationship to the systolic and diastolic works of the heart.

2. Role of the conicity index in reflecting the regional changes in the LV geometry.

3. Role of the Selvester QRS score to determine the extent of myocardial scar in patients with anterior MI and its relation to LV remodelling.

CHAPTER TWO

REVIEW OF LITERATURE

CHAPTER TWO

REVIEW OF LITERATURE

2.1. Myocardial infarction

2.1.1. Definition and cause:

Myocardial infarction is defined as cardiac ischemia produced from a decrease or absence of blood perfusion, this usually results from a blood clot in the coronary artery that supplies that region of the heart muscle. The severity of MI differs relying on the size of the infarcted lesion, the extent of coronary artery occlusion, and the number of collateral arteries (Heusch & Gersh, 2017).

It is now documented that, not all cases essentially require a blood clot for its occurrence, in all living tissue such as the heart muscle, the blood supply necessity equals the oxygen demands of the muscle, this is called the supply–demand ratio. An inequality in this ratio (too slight supply or too much demand) as might occur with a very fast heart rate (too much demand) or a fall in blood pressure (too little supply) may lead to myocardial damage without the presence of a blood clot (Saleh & Ambrose, 2018).

Myocardial infarction induces by: displaced blood clots and embolism, inequity between the demand and supply of blood to the heart muscle, percutaneous interventions, atherosclerosis caused by stents, subsequent to coronary artery bypass surgery (Anderson & Morrow, 2017).

Any one of the following criteria meets the diagnosis for old MI: 1) Pathological Q waves, with or without symptoms, in the absence of non

ischemic causes. 2) Imaging evidence of loss of viable myocardium in a pattern consistent with ischemic etiology (Thygesen *et al*., 2018).

The electrocardiographic (ECG) changes associated with prior anterior MI include: any Q wave in leads V2–V3 >0.02 s or QS complex in leads V2–V3, or Q wave ≥0.03 s and ≥1 mm deep or QS complex in leads V4 (Thygesen *et al*., 2018).

2.1.2. Epidemiology of myocardial infarction:

The average age of the first MI is 65.6 years for males and 72.0 years for females, MI is widespread among older adults (Moore *et al*., 2021). The annual occurrence of MI is about 605,000 new cases and 200,000 recurrent cases and it happens once every 40 seconds in the U.S. (Benjamin *et al*., 2019; Moore *et al*., 2021). The prevalence of MI is about 3.0% for U.S. adults aged 20 years and older (Benjamin *et al*., 2019).

The epidemiological data on the occurrence and prevalence of coronary artery disease in Iraq are restricted owing to the absence of evidence based national guidelines for the management of cardiovascular disease and surveillance studies as compared to other Eastern Mediterranean countries (Traina *et al*., 2017), but there was a study conducted in Albasrah in Al-Sadr Teaching Hospital to assess the mortality of MI in the cardiac care unit the study showed the death rate in hospitalized patients was 16.5% (Al-Asadi & Kadhim, 2014).

A retrospective study done in Romania to evaluate an unknown mortality database involved all deaths recorded in Romania during 1994–2017, using the data from the death record the result exhibited that MI was recorded as the essential reason of death for 501,796 cases (8% of

total deaths). 39.3% of total MI deaths occurred in women and 60.7% in men. MI mortality rate per 100,000 person/years was 98.5 (Ioacara *et al*., 2020).

2.1.3. Risk factor:

A number of relevant studies were conducted in Iraq. In Alsulaimania and Erbil two studies were performed to assess the prevalence of the most frequent risk factors for acute myocardial infarction (AMI) in Iraqi patients the studies showed: A sedentary lifestyle among MI patients was (81.8%-85.1%), (61%-74.3%) were hypertensive and (20%-29.7%) were diabetic. The prevalence of Body mass index (BMI) > 25 was (35.1%). Current, passive, and ex- smoking was (39.2%-69.7%). 51.4% of the AMI patients had a positive family history of coronary artery disease. A greater incidence of MI in male patients compared to females. Myocardial infarction was lesser among the patients from rural regions than among those from urban regions. The prevalence of dyslipidemia was (39.4%-41.2%). High level of low density lipoprotein (LDL) was found in 50% of patients, high triglycerides in 41.9%, low high density lipoprotein (HDL) in 39.2%, and high total cholesterol in 34% (Amen *et al*., 2020; Sharif & Lafi, 2021).

Another study conducted in Babylon showed that most patients have no physical activity (86% of males and 98% of females). 80.56% of males and 71.42% of females were hypertensive. 64.81% of males and 66.67% of females were diabetic. While the percentage of smokers was high (60% of males and 21% of females). The incidence of BMI > 25 was 13.9% in males and 21.4% in females (Dawood, 2015).

The occurrence of first MI in women 6–10 years later than in men owing to defending effect of their natural estrogen before menopause. Female

sex hormones have been associated with a reduction of LDL and an increase in HDL (Rørholm *et al*., 2016).

A study done by Andersson and Vasan (2018) about the epidemiology of cardiovascular disease in young persons showed the proportion of substance abuse (opioids, cocaine, electronic cigarettes, and anabolic steroids) is rising among young adults, which may lead to the incidence of AMI.

2.2. Adverse left ventricular remodelling:

Left ventricular adverse remodelling is a complex process marked by morphological alteration of LV structure and shape resulting from cardiac injury and also leading to changes in cardiac function (Reindl *et al*., 2019).

Left ventricular remodelling is an active process that develops quickly within days or weeks following infarction, if the LV tends to become a spherical shape early after MI the spherical transformation depends on the enlargement of the non-infarcted parts. This change occurs within the weeks or months after infarction. Therefore, the evaluation of LV sphericity within the first days following MI might be too early (Pezel *et al*., 2020).

The risk of heart failure (HF) is 2.7 times greater in patients with LV remodelling compared with those without LV remodelling (van der Bijl *et al*., 2020).

2.2.1. Mechanism of Adverse Remodelling:

Myocardial infarction occurs as a result of occlusion of coronary arteries, under an ischemic condition, cardiac myocytes undergo an

anaerobic metabolism with the instability of the cell membrane so, cell death by apoptosis, autophagy, and necrosis (Heusch & Gersh, 2017; Curley *et al*., 2018).

Ischemic necrosis causes the death of millions of cardiac myocytes concurrently, which leads to an influx of inflammatory cells including macrophages and other antigen-presenting cells into the infarcted area. This leads to the destruction of the collagen scaffolding that helps to maintain ventricular shape leading to regional thinning and dilation of the myocardium in the infarcted areas, this process changes the ventricular shape. When the inflammatory response reaches its maximum, scar tissue is made as a consequent of the direction of fibroblast to the infarcted region to form a new collagen matrix (Bhatt *et al*., 2017).

Following the ischemic event, the inflammation may continue for a variable duration of time, owing to persistent stress on the myocardial wall. The apoptotic alterations are significantly intensified by fibrosis that results from the compensatory activation of two major neurohormonal systems, the SNS and the RAAS. All of these processes lead to alterations in the cardiac architecture and geometry, which are called adverse ventricular remodelling that lead to a higher incidence of HF and death (Curley *et al*., 2018).

The infarcted part is expanded owing to an absence of balancing of the forces created by the normally contracting myocardium, as a result, the increased wall tension causes thinning of the infarcted wall and the extension of the MI in the neighboring areas. Furthermore, the stretched infarcted tissue increases the LV volume with a combined volume and pressure overload on the non-infarcted zones. In situations of increased workload, the normal cardiac myocytes will stretch and gradually

hypertrophy to preserve a normal stroke volume with a reduced number of correctly performing myocardial parts (Zhang *et al*., 2005). Lastly, overstretching will lead to the missing of the compensatory Frank-Starling mechanism and finally result in LV dilatation (Frantz *et al*., 2022). **Figure (2-1).**

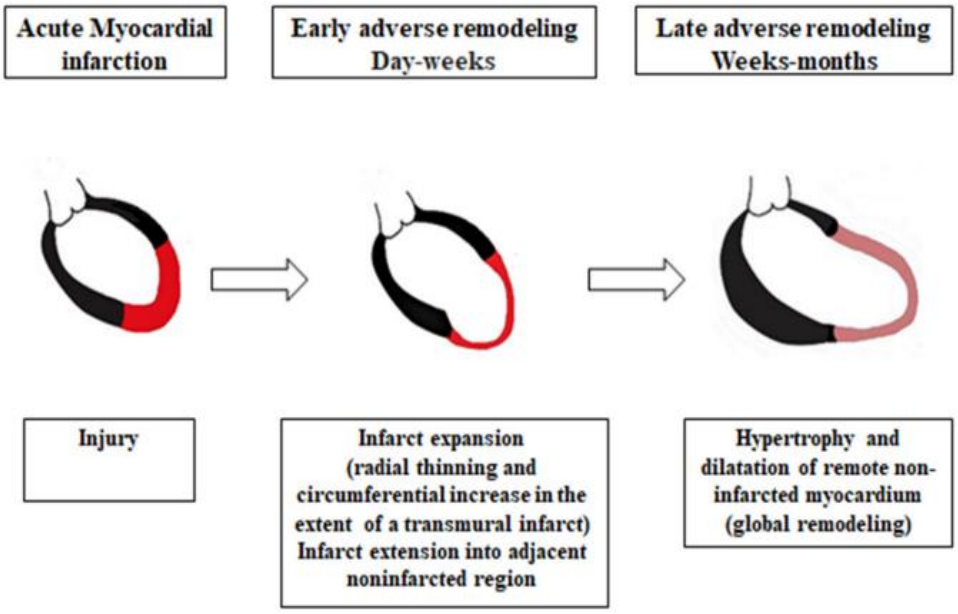

Figure (2-1) Mechanism of adverse left ventricular remodelling (Leancă *et al*., 2022).

2.2.1.1. Neurohormonal regulation:

The main cardioregulatory hormones involved in the process of LV remodelling include the SNS and the RAAS, neurohormones act as important regulatory pathways for the progress of adverse ventricular remodelling, and act as pharmacological targets for the inhibition of adverse remodelling and enhance reverse remodelling (Bhatt *et al*., 2017).

The β-adrenergic tone that is produced from the SNS causes an increase in heart rate and stroke volume, continuous sympathetic activation may lead to harmful effects on the LV. Progressive SNS over activity can

weaken excitation-contraction coupling and then reinforce apoptotic pathways, as well as, chronic catecholamine activity may impair cardiac function, and stimulate fibrosis (Osadchii *et al*., 2007).

Angiotensin II plays an important role in vasoconstriction and aldosterone release, it is also produced in the infarcted heart. Locally created angiotensin II motivates transforming growth factor-β1 production, which in turn, enhances the proliferation and collagen generation of myofibroblast, and results in cardiac fibrosis (Garza *et al*., 2015).**Figure (2-2).**

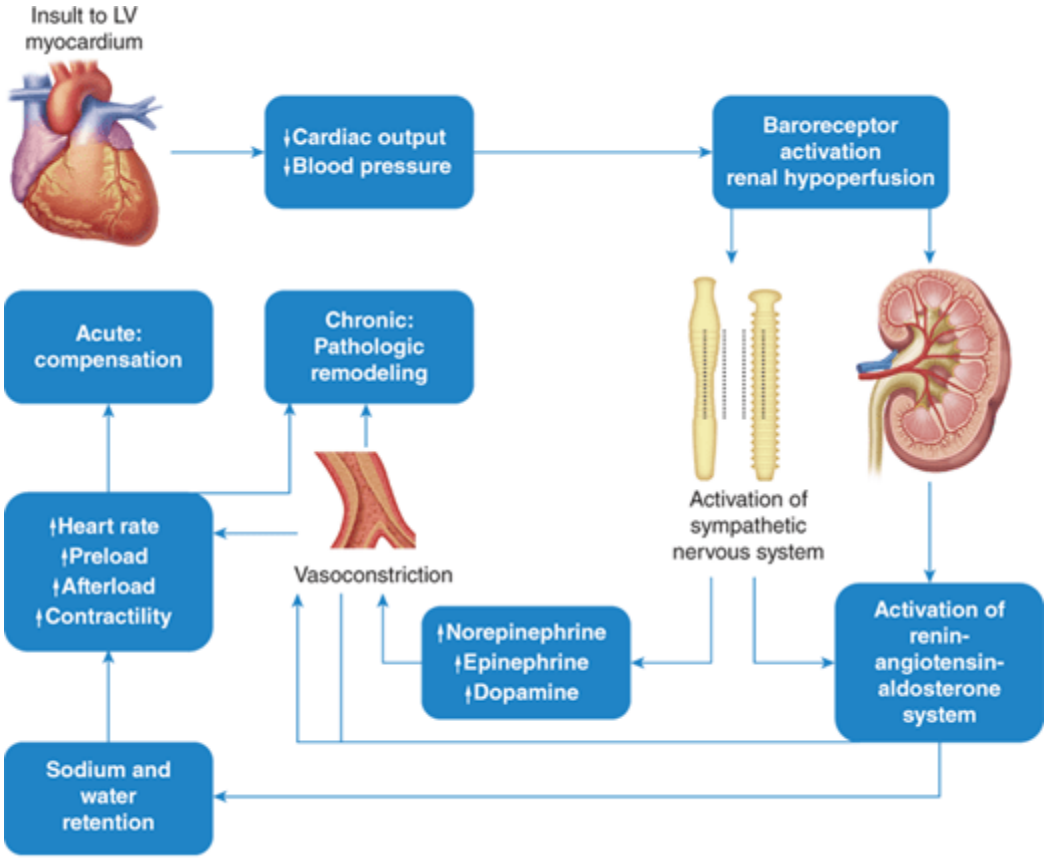

Figure (2-2) Neurohormonal regulation after myocardial infarction (Baliga & Abraham, 2018).

2.2.2. Predictor of left ventricular remodelling:

The important predictor of left ventricular remodelling is infarct size, patients who suffer from ST-segment elevation myocardial infarction (STEMI), which creates infarct scars with a transmural extent, generally develop ventricular remodelling (Masci *et al*., 2011).

As infarct size represents a predictor of LV remodelling, its incidence is greater among patients without any effective reperfusion. Anterior MI and higher serum troponin T levels also represent predictors of adverse LV remodelling (Chew *et al*., 2018).

In addition to that, elderly patients, and myocardial hemorrhage also forecast LV remodelling. The irreversible patterns of ischemia-reperfusion damage of the cardiac microvasculature which are microvascular obstruction and intramyocardial hemorrhage also predict remodelling, intramyocardial hemorrhage causes deterioration of the systolic dysfunction of infarcted parts, enhances infarct expansion, and results in ventricular enlargement (van der Bijl *et al*., 2020).

2.3. Echocardiography

2.3.1. Definition:

Echocardiography plays an important role in the diagnosis and evaluation of cardiovascular disease. The severity of the disease, its progression over time, and the selection of the best therapy can be determined by echocardiography. The usage of echocardiography persists in growing, not only in number but also in the types of measurements, from M-mode to two-dimensional imaging, doppler echocardiography, three-dimensional imaging, and speckle-tracking (Papolos *et al*., 2016).

Echocardiography is low-cost, without radiation, a suitable technique, and broadly used for noninvasive examination of LV structure and geometry in patients with heart disease, with real-time visuals, compared with magnetic resonance imaging (MRI) and computed tomography (Kalogeropoulos *et al*., 2012). Assessment of ventricular remodelling depends on measuring ventricular geometry and function, which can be done by echocardiography or cardiac magnetic resonance (CMR) (Boulet & Mehra, 2021; Frantz *et al*., 2022).

Echocardiography can give rise to significant information during the whole patient pathway, also represent a cause for changes in medical therapy in 60–80% of patients in the pre-hospital setting, increase diagnostic precision and proficiency in the emergency room (Lancellotti *et al*., 2015).

2.3.2. The principle of echocardiographic work:

Ultrasound transducers work using the piezoelectric effect. When an electrical voltage is applied, the piezoelectric crystals alter their shape, thus a varying voltage can make them oscillate rapidly, therefore producing ultrasound. Also, if the returning ultrasound wave oscillates the piezoelectric crystals, they produce an electrical voltage that can be revealed as a signal. So the crystal acts as a generator and detector for ultrasound.

The ultrasound wave encounters tissues of different characteristics and densities, parts of the wave are transmitted, reflected, and refracted. The parts that are transmitted pass in a straight line, the part that is passed through the different mediums will be refracted through the tissue, while the part that is not absorbed by the tissues will be reflected and then go back to the wave's origin (Le *et al*., 2016).

A two-dimensional echocardiography (2DE) transducer is composed of multiple piezoelectric elements ranked in a single row and insulated electrically from each other. By firing individual elements, individual ultrasound waves are produced. The linear array can be steered in two dimensions vertical and lateral.

A three-dimensional echocardiography (3DE) transducer is composed of about 3000 independent piezoelectric elements, which are arranged in rows and columns and used to steer the beam electronically. This ranking of piezoelectric elements permits their phasic firing to produce an ultrasound beam that can be steered in vertical, lateral, and anteroposterior directions to acquire a volumetric (pyramidal) data set (Badano, 2014). **Figure (2-3)**.

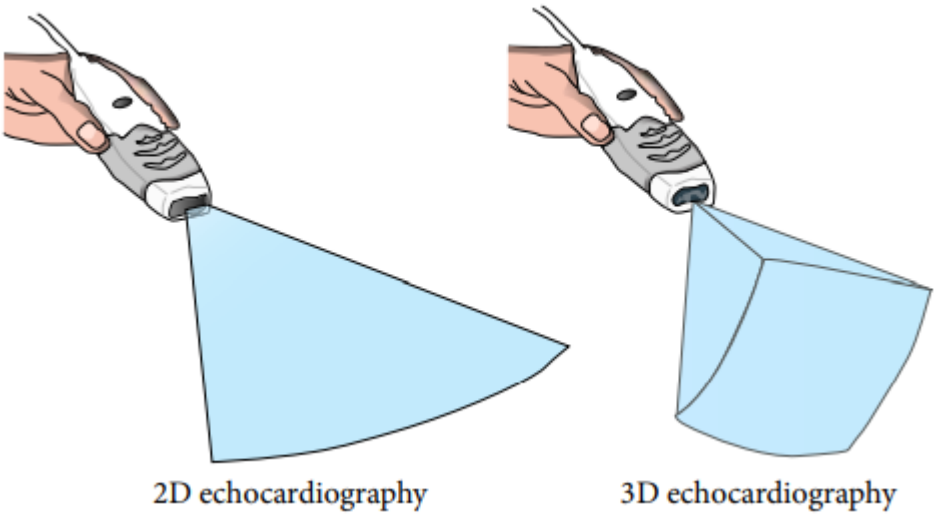

Figure (2-3) Two-dimensional and three-dimensional echocardiographic transducers (Badano, 2014).

2.3.3. Two-dimensional echocardiography:

Two-dimensional echocardiography represents the most recursive imaging method used to assess LV size and function, 2D echocardiography is considered the principal method to reveal remodelling by identifying contractile dysfunction and bi-ventricular geometry (Lang *et al*., 2015).

The information provided by 2DE predicts cardiovascular disease, and the morphological and functional features of the left ventricle are effectively assessed by 2DE. It facilitates the estimation of EF using the measured left ventricular volumes (Jan & Tajik, 2017).

It can also assess valvulopathies and their reason, such as tethering in secondary mitral regurgitation (MR), which is indicative of adverse remodelling (Boulet & Mehra, 2021).

2.3.4. Three-dimensional echocardiography:

Three-dimensional echocardiography has been confirmed to be more precise, doesn't depend on geometric assumptions about LV shape, and has additional value for outcome prediction as compared with 2DE, to get an early discovery of myocardial dysfunction before any obvious decrease in left ventricular ejection fraction (LVEF), 3DE has raised interest lately to detect myocardial deformation (Rodríguez-Zanella *et al*., 2019).

For measuring of LVEF in patients with critical range values (between 30% and 40%), to choose the best treatment, 3D echocardiography is the favorite method (Galderisi *et al*., 2017).

In 2012, recommendations were posted to supply physicians with a systematic approach to 3D echo data set acquisition and analysis (Lang *et al*., 2012). In 2015, an update of the recommendations for cardiac chamber quantification using echocardiography recommended 3DE for precise measuring of left and right ventricular size and function (Lang *et al*., 2015).

Three dimensional echocardiography is rapidly considered the method of choice superior to 2DE. At present time the technology is still being refined so it is used to complement 2DE (Jan & Tajik, 2017).

Owing to its factual imaging of natural valves and their anatomic relationships, better geometric quantification of the valve, and enhanced reproducibility of disease severity outcomes, 3DE is considered better than 2DE and it also offers supplementary information compared to 2D echocardiography when evaluating valvulopathies (Frantz *et al*., 2022).

2.3.4.1. Advantages and limitations of three-dimensional echocardiography:

The most important benefit of the 3D echo is that a full volume dataset can be acquired in three dimensions. Along with image cropping and rotation, views of heart structures can be attained, permitting more anatomically orientated views and simple comprehension by cardiac surgeons and interventional cardiologists (Poon *et al*., 2019).

Among the advantages of 3DE over 2DE are better evaluation of the cardiac volumes and function, and a better view and valuation of valve dysfunction (Tanabe, 2020).

It can be said that the appearance of 3DE is the most important technical progression in ultrasound imaging over the past two decades. One of the

most important distinctive qualities of the new 3DE systems is their capacity to image cardiac anatomy and function from any number of spatial view planes. Consequently, the quantification of LV geometry is bettering, the 3D echocardiography does not rely on geometric assumptions (Lang *et al*., 2012).

Among the restrictions of 3D echocardiography are the need for regular rhythm, low temporal and spatial resolution, and time consuming offline analysis (Lang *et al*., 2012). The image finesse of 3D echo is reliant on that of 2D echo being exposed to the same type of artifacts as verbalized by the physics of ultrasound (Poon *et al*., 2019).

2.3.5. Echocardiographic assessment of left ventricular remodelling:

2.3.5.1. Sphericity index:

The left ventricular sphericity index (SI) is an indicator of LV remodelling and an underused measurement of LV geometry, that can be easily attained from standard echocardiographic images. SI has been regarded as an independent forecast of left ventricular remodelling and recurrent HF. Greater SI was a predictor of mortality and heart failure following AMI (Anvari *et al*., 2018).

Choi *et al*. (2015) made a study of the impact of surgical ventricular reconstruction on sphericity index in patients with ischaemic cardiomyopathy, and found that an increase in SI was associated with poorer survival in patients with ischaemic cardiomyopathy and with anterior wall akinesia or dyskinesia undergoing surgical revascularization. SI represents a ratio of the LV short axis to the long axis dimension.

2.3.5.1.1.Sphericity index by three-dimensional echocardiography:

A study was done by Ola *et al*. (2018) to detect left ventricular remodelling in acute STMI after primary percutaneous coronary intervention (PCI) by 2DE and 3DE. The study demonstrates that 3D-SI has been related to the incidence of LV remodelling. In contrast to the 2D sphericity index, the 3D-SI can predict precisely and early in the subacute phase after an AMI which patient is probably to develop LV remodelling. It is considered the most powerful predictor of remodelling between clinical, electrocardiographic, and echocardiographic parameters. The resolution, rapidity, and predictive value of 3DE make it the perfect technique for evaluation, risk stratification, and monitoring after AMI. The geometric modification of the LV can be assessed by 3DE through the measurment of the 3D sphericity index (3D-SI).

The three-dimensional sphericity index of the left ventricle represents the ratio between the left ventricular end diastolic volume (LVEDV) to the hypothetical sphere volume (Vieira *et al*., 2013)**. Figure (2-4)**.

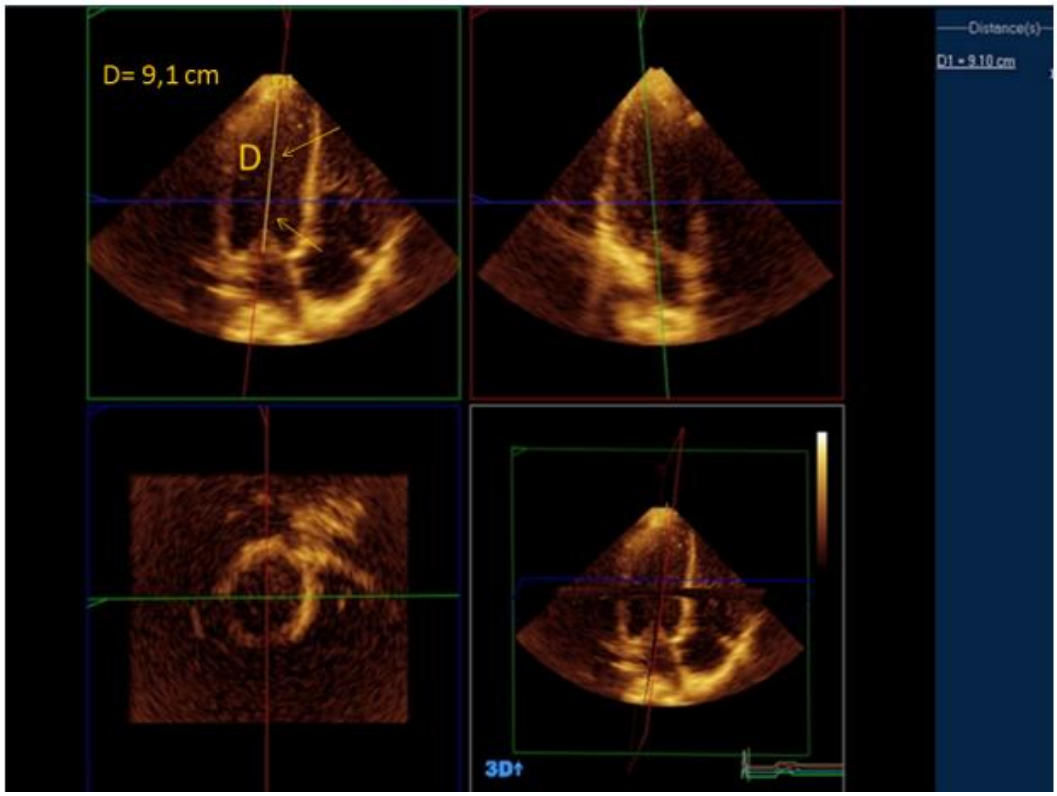

Figure (2-4) Measurement of the three-dimensional sphericity index. The LV cavity is shown, of which D is the LV end-diastolic major long axis. With the formula: $(4/3 * \pi * (D/2)^3)$ a spherical volume in mL can be calculated. The 3D sphericity index is calculated as $EDV/(4/3 * \pi * (D/2)^3)$ where $\pi = 3.14$ (Vieira *et al*., 2013).

2.3.5.2. Conicity index:

The conicity index is the ratio between the apical axis and the short axis of the left ventricle, which measures the apical shape as shown in **figure (2-5)**. It is extremely associated with the location of the previous infarct. A study that measured CI in patient with ischemic cardiomyopathy, revealed that the CI tends to be greater when the lesion is an anterior infarct (Garatti *et al*., 2015).

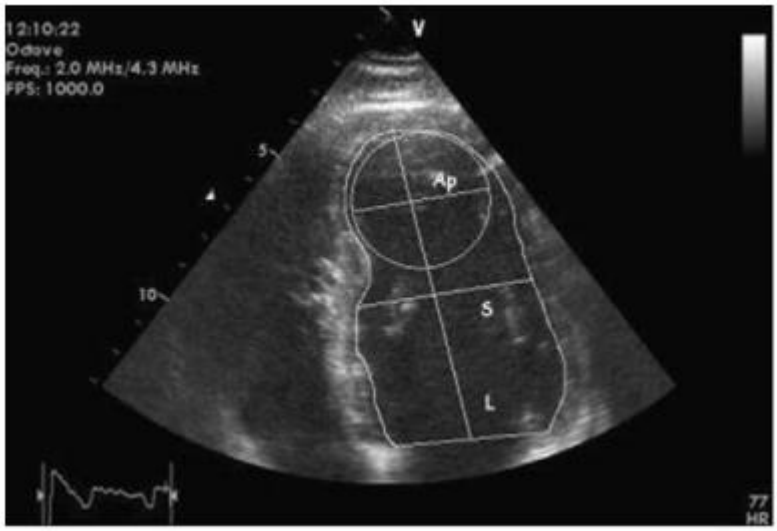

Figure (2-5) Four chamber view used to measure the apical axis(Ap) at end diastole. Where (S) short axis, (L) long axis (Di Donato *et al*., 2006).

A higher SI represents a more spherical LV shape, and an increased CI indicates apical regional dilatation, which is repeatedly noticed in ischemic cardiomyopathy patients (Oh *et al*., 2013).

Fan *et al*. (2010) considered the CI as an index on left ventricular apical geometry after myocardial infarction using CMR, and they demonstrated that the regional left ventricular abnormalities, particularly in patients with a left ventricular aneurysm that developed after MI can be assessed by using the CI.

A study done by Kaolawanich and Boonyasirinant (2019) to evaluate the usefulness of the apical area index to predict left ventricular thrombus in patients with systolic dysfunction by CMR, the study revealed that 50% of patients with LV thrombus had an apical aneurysm which was a significant predictor of severe apical a synergy. Patients with LV thrombus had a considerably higher apical area index than those without thrombus. The apical area index represents a predictor of LV thrombus formation from CMR in patients with systolic dysfunction.

2.3.5.3. Diastolic function

At the end of systole, sudden untwisting happens, allowing the pressure inside the LV to fail, which permits the opening of the mitral valve and blood flows along a negative pressure gradient toward the apex until the pressure is balanced between the left atrium (LA) and the LV resulting in diastasis, then atrial contraction occurs which represents the last stage in the ventricular filling, imbalance in any of these stages may lead to diastolic dysfunction (Oktay *et al*., 2013).

The four stages of diastole include isovolumic relaxation, rapid filling (represented by E mitral inflow wave), slow filling (diastasis), and active filling (represented by A mitral inflow wave). Passive filling occurs when the LV is filled with blood first by a pressure gradient between the left atrium and the left ventricle. Active filling occurs when the atrium is contracted which permits ventricular filling at the end of diastole (active filling) (Kossaify & Nasr, 2019).

The chief parameters for evaluation of LV diastolic function comprise mitral flow velocities, mitral annular e′ velocity, E/e′ ratio, peak velocity of tricuspid regurgitation (TR) jet, and left atrial volume index (LAVI).

By tissue Doppler imaging, e′ and E/e′ ratios are used to measure longitudinal fiber lengthening during early diastole at the level of the mitral valve annulus. The e′ maximal velocity represents the LV relaxation rate, while E/e′ reflects the LV filling pressures (Mitter *et al*., 2017).

While relaxation in early diastole appears as an e′ wave, the a′ wave occurs owing to the atrial contraction in late diastole, e′ is influenced by LV elastic recoil, the lesser the LV end systolic volume, the faster the recoil, and the greater e′ (Popović *et al*., 2011).

2.3.5.3.1.Diastolic dysfunction:

The initial common change in several cardiovascular diseases is left ventricular diastolic dysfunction (LVDD), with a prevalence rate ranging from 3% to 39%. Diastolic dysfunction (DD) evaluated using echocardiography has been demonstrated to be a strong predictor of survival after MI, independent of indicators of left ventricular size and systolic function, in addition to relevant clinical factors (Prasad *et al*., 2018).

LVDD causes elevated LV filling pressures, which occur due to increased chamber stiffness, reduced restoring forces, and decreased left atrial function and LV relaxation (Mitter *et al*., 2017).

decreased E/A ratio<0.8 reveals the compensatory increase in the late atrial filling when the LV fails to relax, principally related to changes in early LVDD (Palmiero *et al*., 2015).

Pseudonormal filling (grade 2 DD) has also been revealed to be independently associated with death, with outcomes similar to those seen with restrictive mitral filling. Little values of tissue Doppler derived mitral annular s' and e′ velocities were independent forecasters of greater risk for death in patients following MI (Biering-Sørensen *et al*., 2014).

Grades of DD were defined according to the 2016 guidelines of the European Association of Cardiovascular Imaging and the American Society of Echocardiography. The four criteria that evaluated LVDD and their cutoff values are as follows: septal e′ <7 cm/s or lateral e′ <10 cm/s, average E/e′>14, LAVI >34 cc/m2, and TR velocity >2.8 m/s.

To evaluate diastolic dysfunction in patients with preserved ejection fraction, four parameters must be assessed: e′, E/e′ ratio, LAVI, and TR velocity (Nagueh *et al*., 2016), as showed in **Figure (2-6)**.

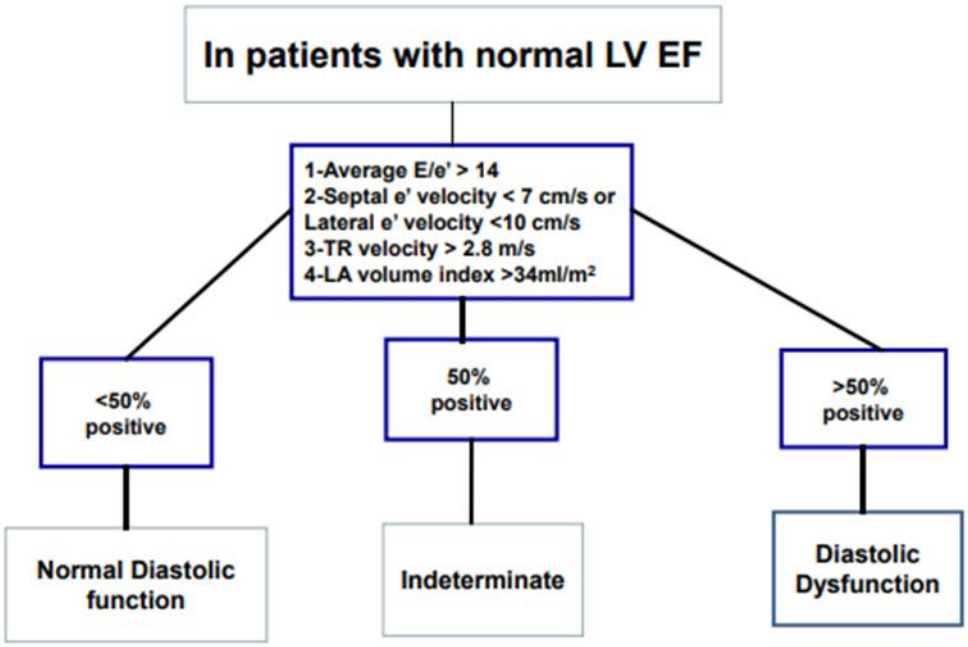

Figure (2-6) Diastolic Function in Patients with preserved left ventricular ejection fraction (LVEF) (Nagueh *et al*., 2016).

Evaluation of Diastolic Function in Patients with decreased LVEF demonstrated in **Figure (2-7)**.

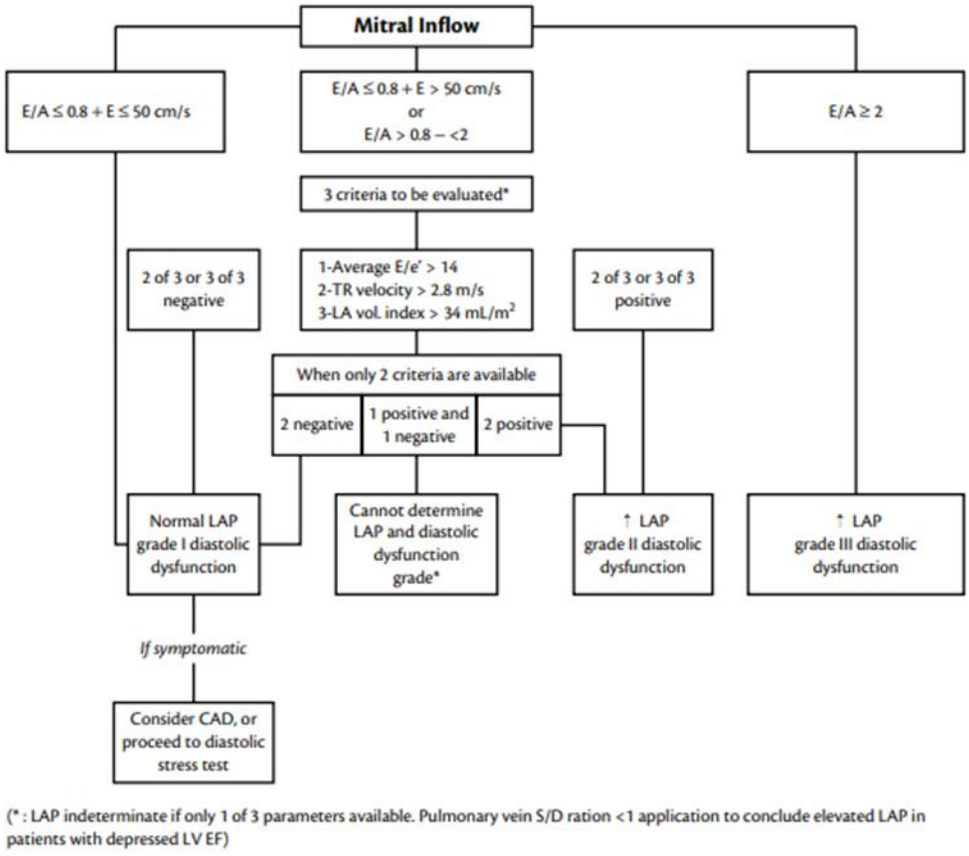

Figure (2-7) Diastolic Function in Patients with decreased left ventricular ejection fraction (LVEF). Where TR velocity (tricuspid regurgitation velocity), LA vol. index (left atrial volume index), LAP (left atrial pressure), CAD (coronary artery disease), (S/D ratio) the ratio between the peak systolic and diastolic velocities (Lancellotti *et al*., 2017).

2.3.5.4. Systolic function:

Ejection fraction is the commonly used and accepted echocardiographic parameter for measuring LV systolic function, and it represents the amount of blood pumped out of the ventricle with each contraction, stroke volume, divided by the end-diastolic volume. This parameter has a distinctive position in cardiology, having served as the criteria of choice

for nearly all therapeutic trials of heart failure, and is well included in clinical guidelines (Ponikowski *et al*., 2016).

The European Association of Cardiovascular Imaging and the American Society of Echocardiography guidelines recommend valuation of LVEF in 2D by modified Simpson's method of discs, obtaining LV volumes from apical 4 and 2 chamber views, or instead if available, by 3D derived full-volume acquisition. Appreciation of LVEF by M-mode can not be used in numerous clinical settings, such as regional wall motion abnormalities and changed ventricular dimensions and geometry, owing to the geometrical assumptions (Lang *et al*., 2015).

There was a strong relationship between 3D echo-derived LVEF and CMR-derived values (Rigolli *et al*., 2016).

LV end diastolic, end systolic volume, and chamber diameters are also indicators of HF and LV remodelling (Curley *et al*., 2018).

2.3.5.4.1. Systolic dysfunction:

A study conducted by Chew and his colleagues to evaluate left ventricular ejection fraction post myocardial infarction found that: Lack of improvement in LVEF was associated with a three fold increased risk of mortality. In the months and years after MI incidence, a greater proportion of patients will develop deteriorated LV systolic dysfunction, which puts them at risk of adverse outcomes including heart failure and sudden cardiac death (Chew *et al*., 2018).

Van der Bijl *et al*. (2020) studied the effect of post infarct left ventricular remodelling on outcomes, and revealed that, in patients with an LVEF<40%, remodelers experienced a higher rate of heart failure

hospitalization in comparison with non-remodelers, and the LVEF was lesser in LV remodelers as compared with non-remodelers.

2.3.5.5. Mitral regurgitation:

When the mechanisms of regurgitation are concerned with the disease of the mitral valve (MV) leaflets or chordae tendineae, then the MR is regarded as primary (Nishimura *et al*., 2014).

Any adverse changes in LV size, shape, or function with or without annular dilatation leading to secondary MR. Following MI, the mitral valve and subvalvular apparatus are affected leading to the development of ischemic mitral regurgitation. Numerous abnormalities can be identified in ischemic mitral regurgitation such as annular dilatation, leaflet tethering with decreased coaptation, and papillary muscle displacement along posterior, apical, or lateral vectors (Nappi *et al*., 2017).

The majority of patients with secondary MR have an enlarged LV with global or regional wall motion abnormalities, and systolic tethering of the leaflets annular, dilation, or both. Severe ischemic mitral regurgitation and LV post infarct remodelling usually occur with a larger infarct size, the incidence of any degree of secondary MR is linked with worsened outcomes in patients with ischemic cardiomyopathy (Nishino *et al*., 2016).

2.4. Electrical conduction system of the heart:

The conduction system of the heart consists of the sinoatrial (SA) node, the atrioventricular (AV) node, the atrioventricular bundle, the right and left bundle branches, and the Purkinje fiber network (Padala *et al*., 2021).

The dominant pacemaker of the heart is the SA node, which controls its rate of contraction. It contains pacemaker cardiomyocytes that can depolarize spontaneously. The action potentials are quickly spread from the SA node to the AV node. Owing to the slow conduction velocity of the AV node, the ventricles fill with blood before the impulse is spread to the ventricles. Then the impulse is quickly spread through the atrioventricular bundle and its branches in the ventricular septum. When the impulse reaches the Purkinje fiber, it is quickly disseminated to the ventricular cardiomyocytes, triggering their contraction (van Eif *et al*., 2018).

2.4.1. Electrocardiography:

Electrocardiography is a device that records the electrical activity of the heart by using electrodes that are applied to the skin. These electrodes detect the electrical changes produced by the depolarization and repolarization of heart muscle (Price, 2010).

Electrocardiography is a reproducible, available, low-cost, and noninvasive diagnostic method that offers risk stratification about myocardial scars (Markendorf *et al*., 2021).

In ECG, the P wave indicates atrial depolarization, the PR interval is the time taken for the impulse to reach the ventricles, the QRS complex indicates depolarization of the ventricles, and the T wave indicates repolarization of the ventricles (van Eif *et al*., 2018).

2.4.2 The Selvester score

2.4.2.1. Definition:

The Selvester QRS score translates subtle changes in ventricular depolarization measured by the electrocardiogram into information about myocardial scar location and size (Loring *et al*., 2011). The Selvester score is an electrocardiogram scoring system derived from changes in Q and R wave duration, R and S wave amplitudes, R/Q ratios, and R/S ratios (Watanabe *et al*., 2016).

It can be measured using modified criteria for each of the following disorders: left bundle branch block (LBBB), right bundle branch block (RBBB), left anterior fascicular block (LAFB), LAFB with RBBB, LV hypertrophy (LVH), and no confounders. The QRS score which consists of 32 points in total represents a collection of criteria that can be drafted to locate and appreciate the degree of myocardial scarring in the left ventricle. Each point constitutes 3% of the myocardial scar area in the left ventricle (Guo *et al*., 2022).

The QRS score has been modified and refreshed several times since its original description in 1972. The most recent update occurred in 2009 with a publication that included a method of application of the QRS score in the presence of hypertrophy and conduction defects (Strauss & Selvester, 2009). Before this study, fascicular blocks, bundle branch blocks, and hypertrophy were excluded and regarded as confounding factors that prevented infarction estimation via QRS score (Loring *et al*., 2011).

2.4.2.2. The Selvester score for estimation of myocardial infarct size:

The selvester score which is calculated from the ECG reflects the extent of myocardial damage in patients with MI (Watanabe *et al*., 2016).

Recent studies used CMR as a standard to appreciate the benefit of the QRS score in locating and evaluating myocardial scars and in measuring the amount of myocardial scarring in the left ventricle. The score properly estimates the area of myocardial scarring regarding the location, type of MI, and type of ECG conduction (Guo *et al*., 2022).

In a study done by Rovers *et al*. (2009) to assess the relationship between the Selvester QRS Score appreciated MI size and contrast-enhanced magnetic resonance imaging's estimated MI size, it was revealed that whether the patients received thrombolytic or not, there were statistically significant correlations between the infarct size assessed by the Selvester QRS Score and the infarct size measured by MRI.

While the use of CMR to risk-stratify patients is promising, it is costly and currently not extensively available so, if QRS scoring can depict the scar size in ischemic and nonischemic cardiomyopathy patients with all types of ventricular conduction, it might have important clinical effects in risk-stratifying patients before implantation of ICD (Strauss & Selvester, 2009).

Watanabe *et al*. (2016) studied the correlation between QRS score and microvascular obstruction in acute anterior MI patients. In comparison with the results derived from CMR imaging, the QRS score may be a better parameter for confirming the presence of microvascular obstruction, even in acute anterior MI patients who have successfully undergone PCI. The estimation of QRS scores just after PCI may be

clinically important to achieve a better prognosis in first-time acute anterior MI patients.

A complete and simplified Selvester QRS score demonstrates comparable predictive value for the evaluation of CMR-derived infarct size and microvascular obstruction in reperfused STEMI (Tiller *et al*., 2019).

In a study conducted by Ciftci *et al*. (2019) to determine the role of selvester score in the detection of left ventricular systolic dysfunction among trastuzumab treated breast cancer patients, they demonstrated that patients with severe left ventricular systolic dysfunction who had myocardial scarring had a statistically significant higher selvester score .

2.4.2.3. The selvestor score predicts cardiac events:

Besides its role in the location and estimation of myocardial scars, the QRS score can also predict some clinical events. The selvestor score and the changes in the selvestor score might be regarded as early predictors for the risk of major adverse cardiovascular events and death in acute STEMI patients who underwent PCI treatment, furthermore, patients who have been subjected to an increase in the selvestor score during treatment with PCI should be cautiously followed up (Liu *et al*., 2020).

QRS scores recognize and measure scars in ischemic and nonischemic cardiomyopathy patients in spite of ECG confounders, greater QRS estimated scar size is associated with an increased risk of arrhythmia (Strauss *et al*., 2008). The QRS score is associated with the risk of ventricular tachycardia, and ventricular fibrillation in nonischemic cardiomyopathy. Therefore, patients with high QRS scores should be treated with extreme caution (Arısoy *et al*., 2021).

In a study of patients with IHD subjected to CMR before ICD implantation, QRS scoring had an important moderate association with CMR estimation of the transmural scar and revealed a correlation with medium term mortality risk. It could be the most suitable for the prediction of death that is not preventable by ICD therapy (Rosengarten *et al*., 2013).

A cohort study was done by Karakuş and Berat (2020) to determine the ability of the selvestor score system to predict rehospitalization in patients with ischemic heart failure. The study involved fifty-four patients with ischemic HF. ECGs were collected on the first day of admission and the Selvestor score was calculated. The result showed that in patients with ischemic HF, ECG estimation of the myocardial scar by selvestor score can be used as a forecaster of re hospitalization, Readmission occurred within the first 3 months, and patients with greater myocardial scar scores have an increased risk of decompensation and rehospitalization.

CHAPTER THREE

PATIENTS AND METHODS

CHAPTER THREE

PATIENTS AND METHODS

3.1. Patients and methods:

3.1.1. Subjects:

This case-control study was conducted in Shaheed Almehrab cardiac catheterization center and Merjan Medical City in Al-Hilla City under the supervision of the physiology department at Babylon Medical College, through the period from September 2022 until February 2023.

The study involved 50 patients (41 males and 9 females), diagnosed with an old anterior myocardial infarction. Another 50 apparently healthy people matching age, sex, weight, and height were included in this study.

3.1.1.1. Sample size calculation:

The sample size was calculated according to the equation below:

$N=Z^2*P(1-P)/d^2$ (Harris *et al*., 2019).

Where:

N: Sample size.

Z: Level of confidence interval which equals to 1.96.

P: The prevalence of myocardial infarction.

The prevalence of myocardial infarction was 3% (Benjamin *et al*.,2019).

d: Estimated error which equals to 5%.

The sample size was 50 cases and 50 controls.

3.1.1.2. Inclusion criteria:

Patients with old anterior myocardial infarction specifically 6 month after MI, ranging in age from 40-60 years and have been diagnosed by a specialized cardiologist.

3.1.1.3. Exclusion criteria:

1. Patients with any type of dilated cardiomyopathy rather than an ischemic cause.

2. Patients with atrial fibrillation and other types of arrhythmia.

3. Patients with poor windows that make 3D assessment difficult.

4. Patients with valvular diseases like aortic regurgitation.

3.1.1.4. Ethical Approval and Consent:

Ethical approval for this project was granted by the Ethics Committee at the University of Babylon College of Medicine, which certified it at 675 on July 21, 2022, and verbal consent was obtained from the participants.

3.1.2. The apparatus:

3.1.2.1 Echocardiography

The study was done using echocardiography (GE Vived E9 XDclear Ultrasound Machine) as shown in **figure (3-1).** 2D, 3D, and Doppler images were acquired) with 3.5-MHz and 4V transducers, made in the Norway by GE Vingmed Ultrasound).

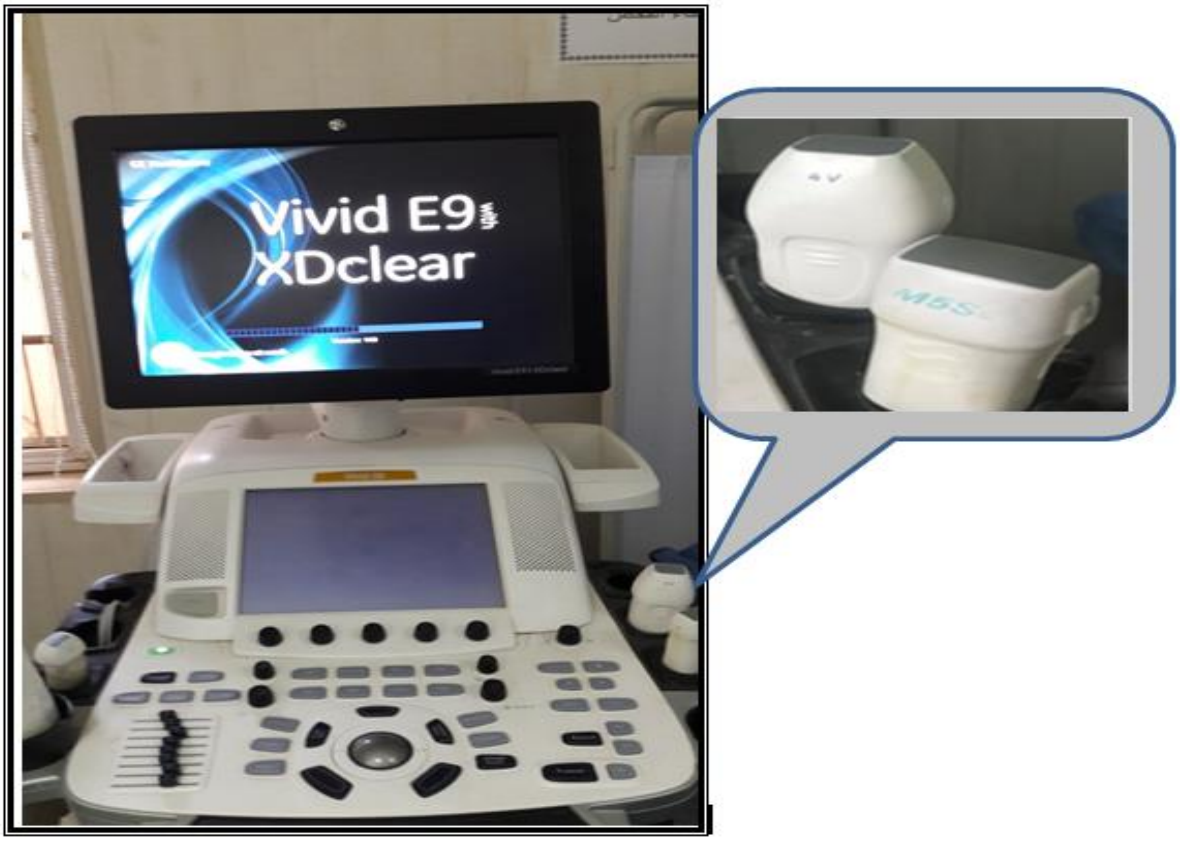

Figure (3-1) Echocardiography machine (GE VIVID E9 XDclear Ultrasound Machine).

3.1.2.2 Electrocardiography

The patients underwent electrocardiography, at a speed of 25 mm/s and an amplification of 10 mm/mV, the ECG was recorded. Ten electrodes were required, six of these were applied to the chest and four were applied to the limbs (Price, 2010).

3.2. Methods

The examination protocol includes

3.2.1. Questionnaire

A self-constricted questionnaire form was prepared by the researcher and supervisor to collect information from the patients after taking their full history about their illness. The questionnaire included information regarding selected variables like sex , age , weight, and height, and then calculated body surface area (BSA) and body mass index (BMI) according to the following equations :

BSA $=\sqrt{\text{Height }(cm)} \times \text{Weight }(Kg)/3600$ (Xiong *et al*., 2022).

BMI = Weight (Kg) / Height² (m²) (Caballero, 2019).

3.2.2. Echocardiographic measurement:

By ECG-guided acquisition, the patients underwent echocardiographic assessment with 2D and 3D modalities .

The patient was instructed to lie on his left lateral position with his left arm placed behind the head and the right arm placed along the right side of the body.

In the apical four chamber view taken at the end of diastole, the long axis was measured from the apex of the LV to the midpoint of the mitral valve, and the short axis was measured from the axis that vertically crossed the midpoint of the long axis. Then 2D-sphericity index was calculated from the ratio between the short axis and the long axis (Di Donato *et al*., 2006). **Figure (3-2)**.

The sphericity index was also calculated by volume ratio, which is the ratio of EDV to the hypothetical sphere volume (EDV/1/6* π*L^3), where L is the long axis of the left ventricle). In the same view, the conicity index was measured, and it represents the ratio between the apical to the short axis, where the apical axis constitutes the diameter of the circle that matches the apex (Di Donato *et al*., 2006), as shown in **figure (3-2)**.

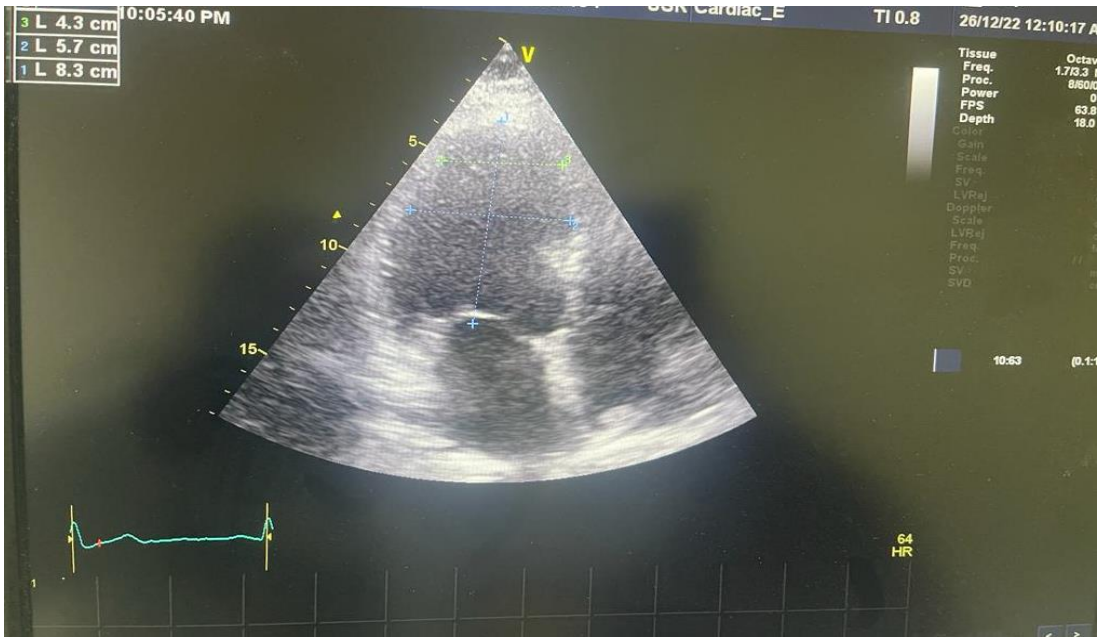

Figure (3-2) Measurement of long axis, short axis, and apical axis in apical four champer view.

The modified Simpson's method was used to compute the left ventricular ejection fraction and left ventricular volumes, end diastole and end systole were identified by assessing the time of the upper and lower limits of the chamber size. In the apical 4-chamber, the endocardial rims were manually selected taking into consideration the inclusion of the papillary muscles and trabeculae in the LV cavity, **Figure (3-3)** (Lang *et al*., 2015).

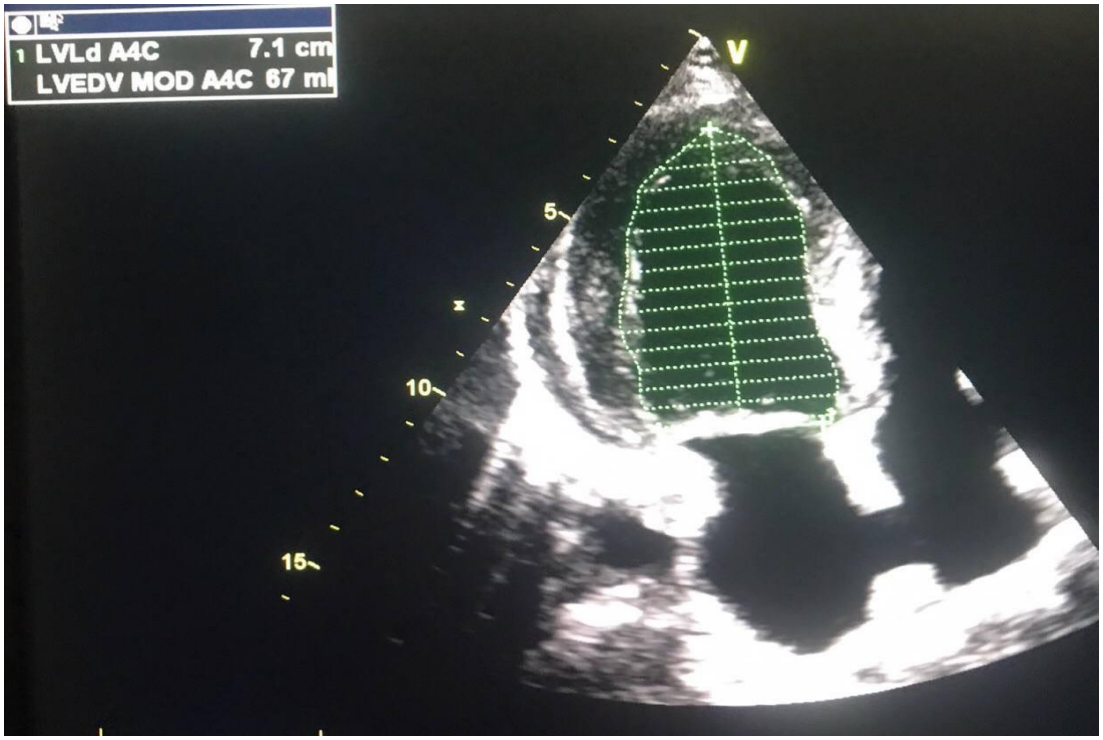

(a)

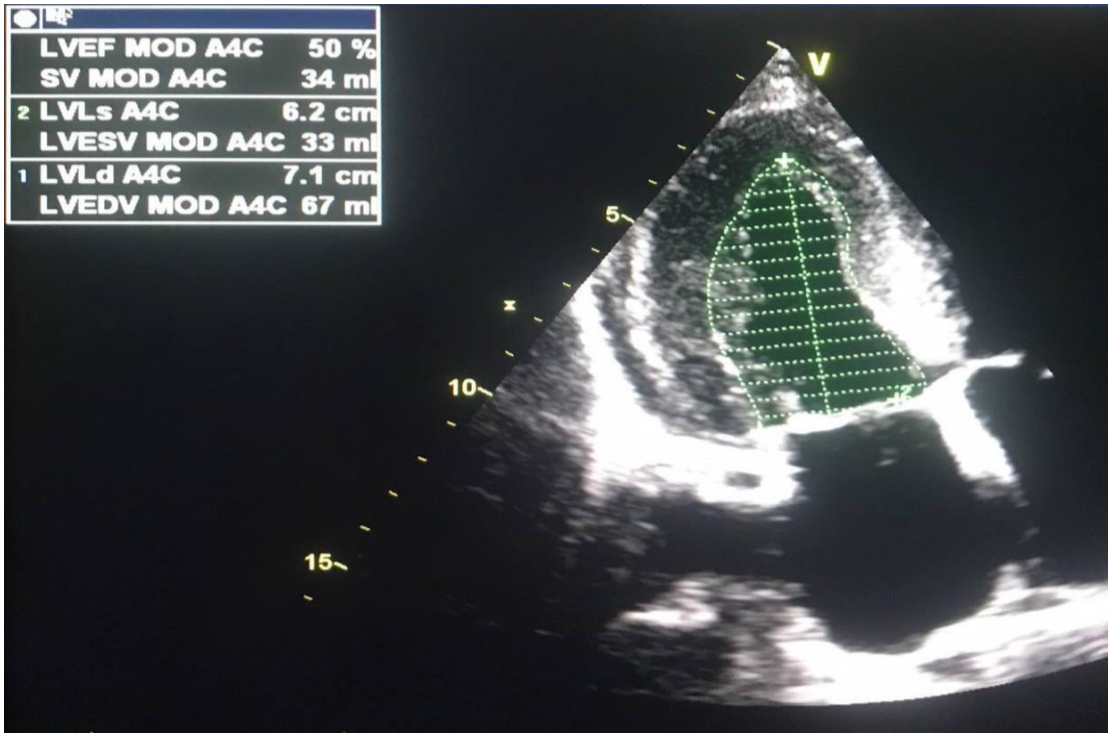

(b)

Figure (3-3) Measurement of ejection fraction by simpson method, (a) at the end diastolic and (b) at the end systolic.

The LA volume was also calculated using Simpson's method, at the end of the systolic phase with the biggest LA volume (Lancellotti *et al*., 2017).

At mid systole, the tenting area of the mitral valve was measured, which represents the area bounded by the valve leaflet tips and annular plane. The tenting height of mitral valve was also measured, which represents the length from the leaflet tips to the annular plane, as seen in **figure (3-4)**, (Matsumura *et al*., 2010).

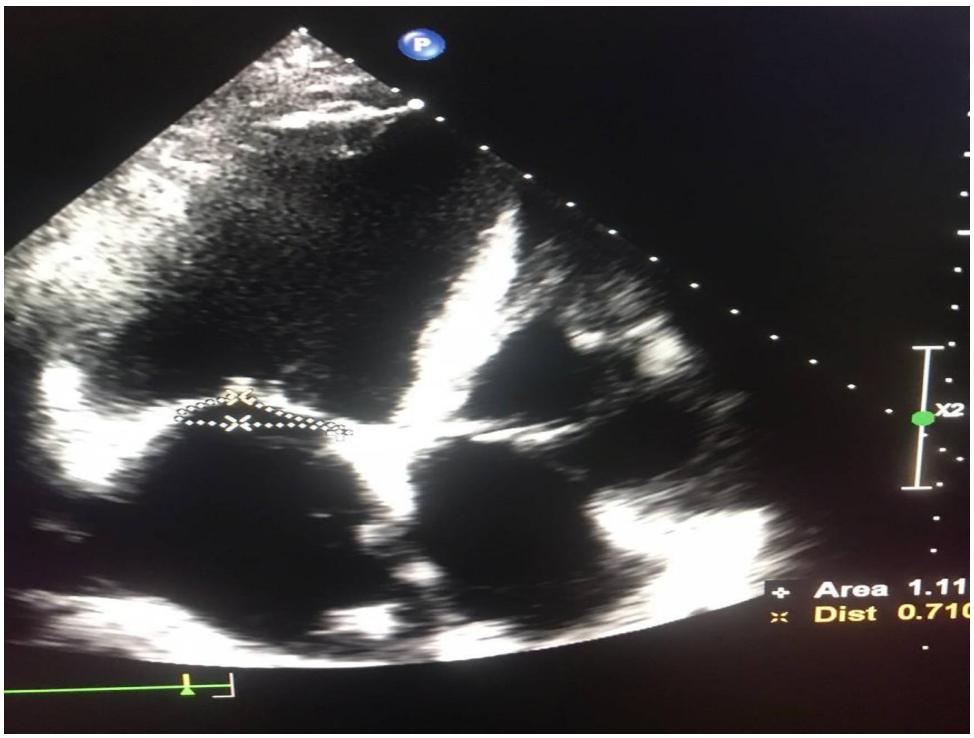

Figure (3-4) Measurement of tenting area and tenting height of mitral valve.

Vena contracta was obtained by using a color doppler on the mitral valve, and measuring the breadth of the jet next to the regurgitant orifice. (Lancellotti *et al*., 2017).

By placing the pulsed wave doppler at the mitral valve leaflet tips, the early (E wave) and late diastolic flow (A waves) was obtained, and the ratio of E/A was measured **Figure (3-5)**. The mean of e' of the medial and lateral sides was computed by tissue doppler imaging, where sample volume was placed at the mitral annulus from both the septal and lateral sides, as seen in **Figure (3-6)**, and the E/e' ratio was calculated (Prasad *et al*., 2018).

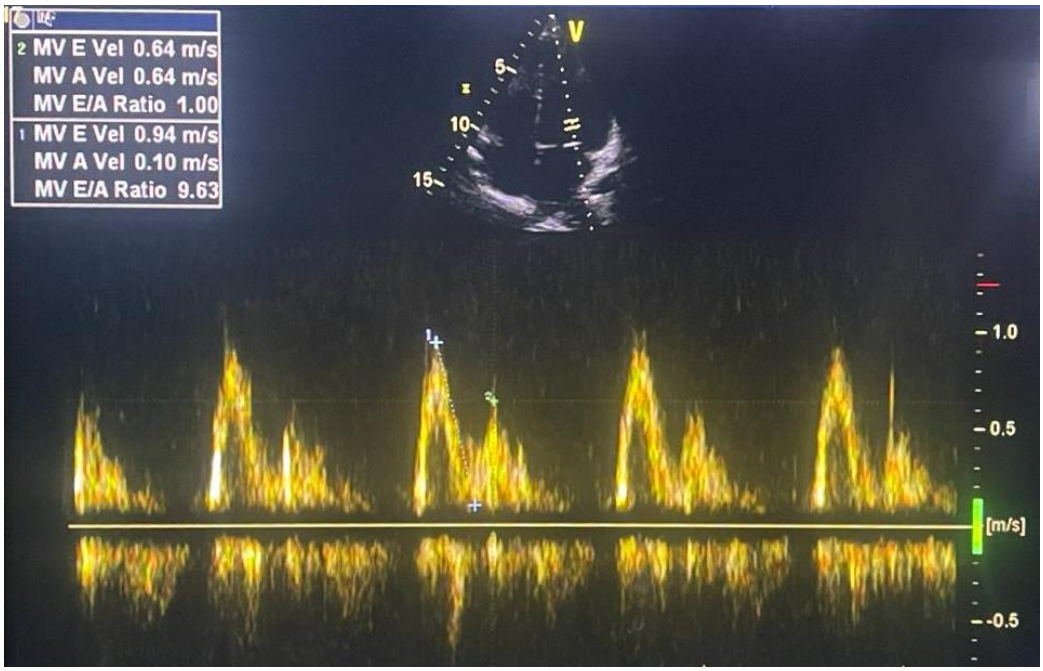

Figure (3-5) Pulsed doppler echocardiography at the mitral inflow shows E/A waves ratio.

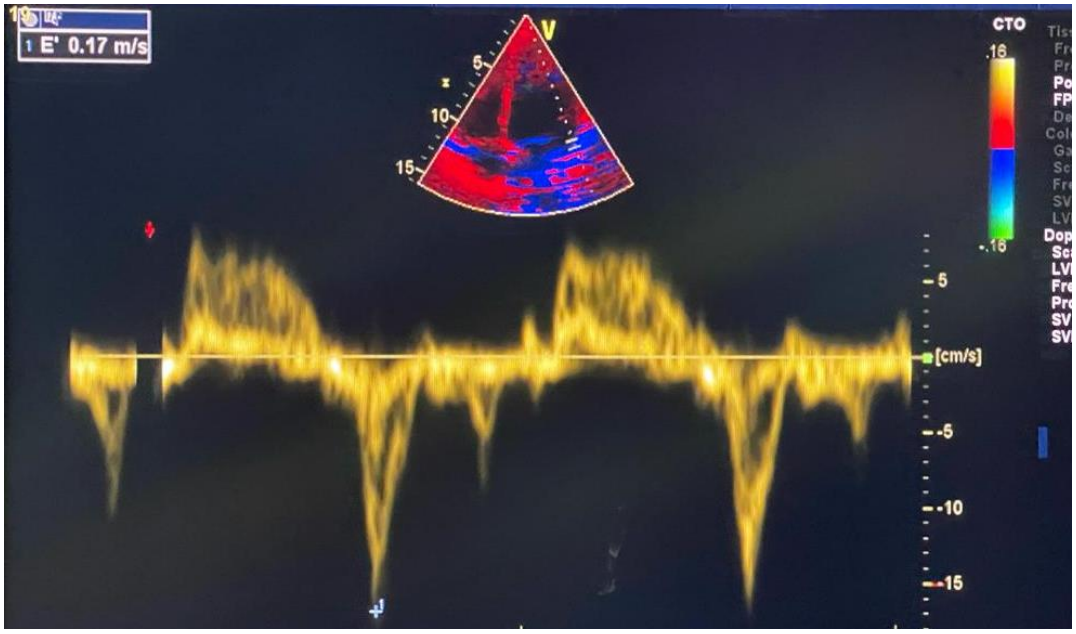

(a)

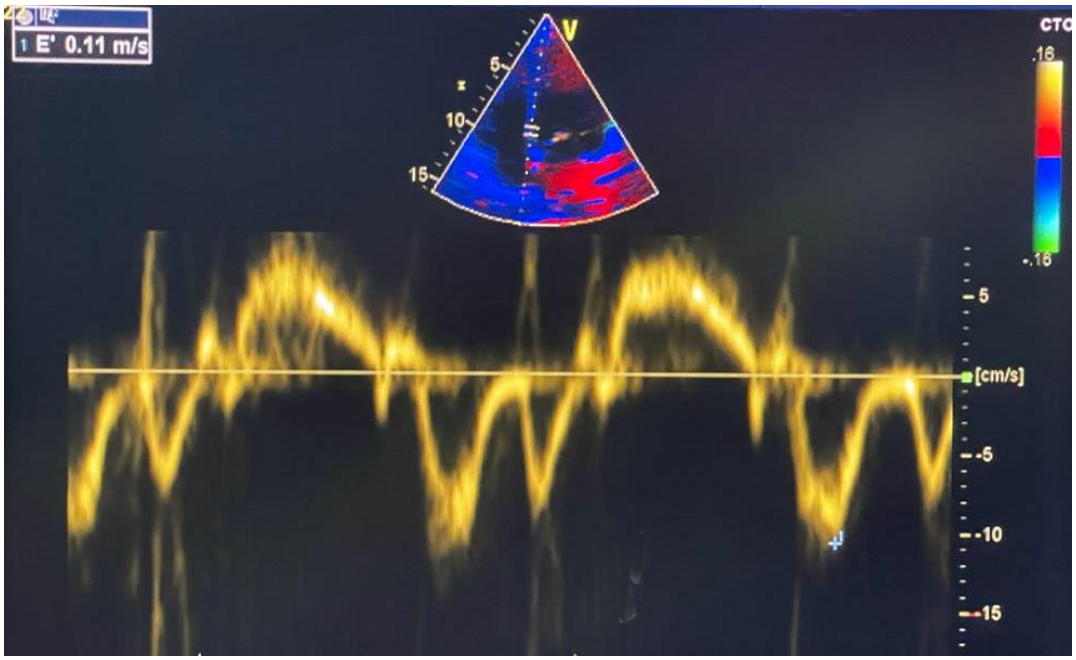

(b)

Figure (3-6) Pulsed tissue doppler imaging (a) at the lateral and (b) at the septal mitral annulus, demonstrate e'.

Tricuspid regurgitant velocity was measured by continuous wave doppler by placing the cursor at tricuspid valve after applying color

doppler to detect the direction of tricuspid regurgitation (Mitchell *et al*., 2019).

Three-dimensional analysis of left ventricular volumes was performed using the 4D Auto LVQ software. After using the 4V transducer, the patient was asked to hold his breath, a full volume dataset over four heartbeats (a multi beat) was used. The mid mitral annular plane and the apex of the LV were manually delineated at both end diastole and end systole. The endocardial border was delineated automatically and altered as needed by adding points, then the LV volumes, EF, SI, and SV were automatically measured. **Figure (3-7)** (Lang *et al*., 2012; Myhr *et al*., 2018).

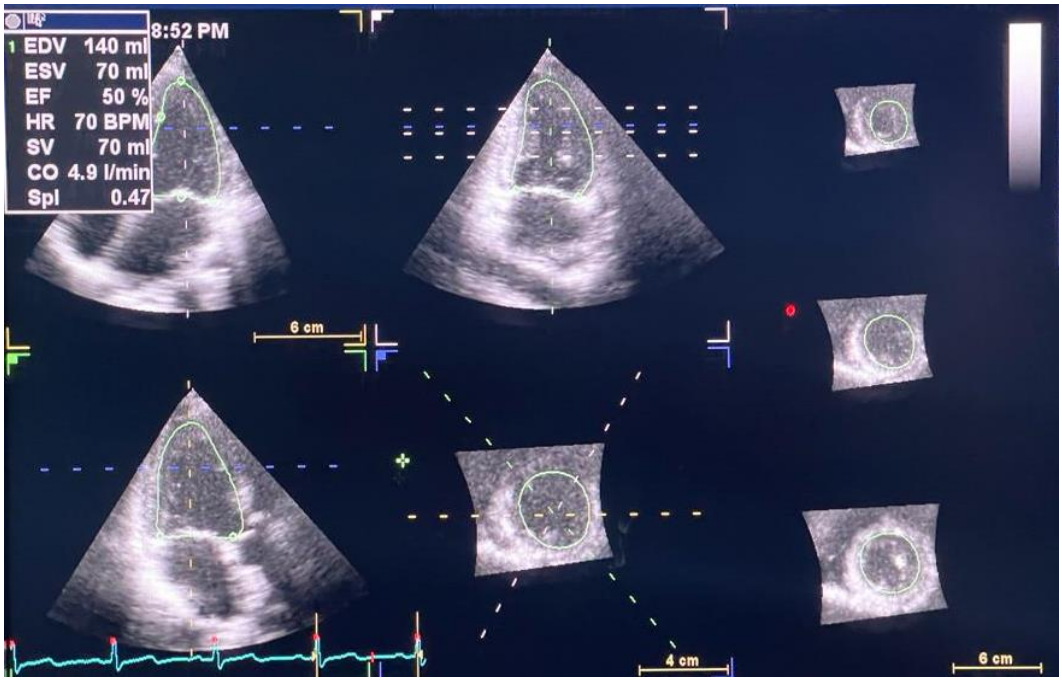

Figure (3-7) Measurement of left ventricular volumes, ejection fraction, sphericity index, stroke volume by three dimension echocardiography.

3.2.3. Performing selvestor scoring:

The patients had an ECG and Selvestor score was calculated as below: Initially, the ECGs were classified according to the type of ventricular conduction or hypertrophy (LBBB, LAFB, LVH, RBBB, RBBB + LAFB, and nonconfounding factors). When lead V1 experienced a negative deflection (rS or Q morphology), the analysis was conducted in accordance with **figure (3-8 a)**, and in accordance with **figure (3-8 b)** when lead V1 experienced a terminal positive deflection (Guo *et al*., 2022).

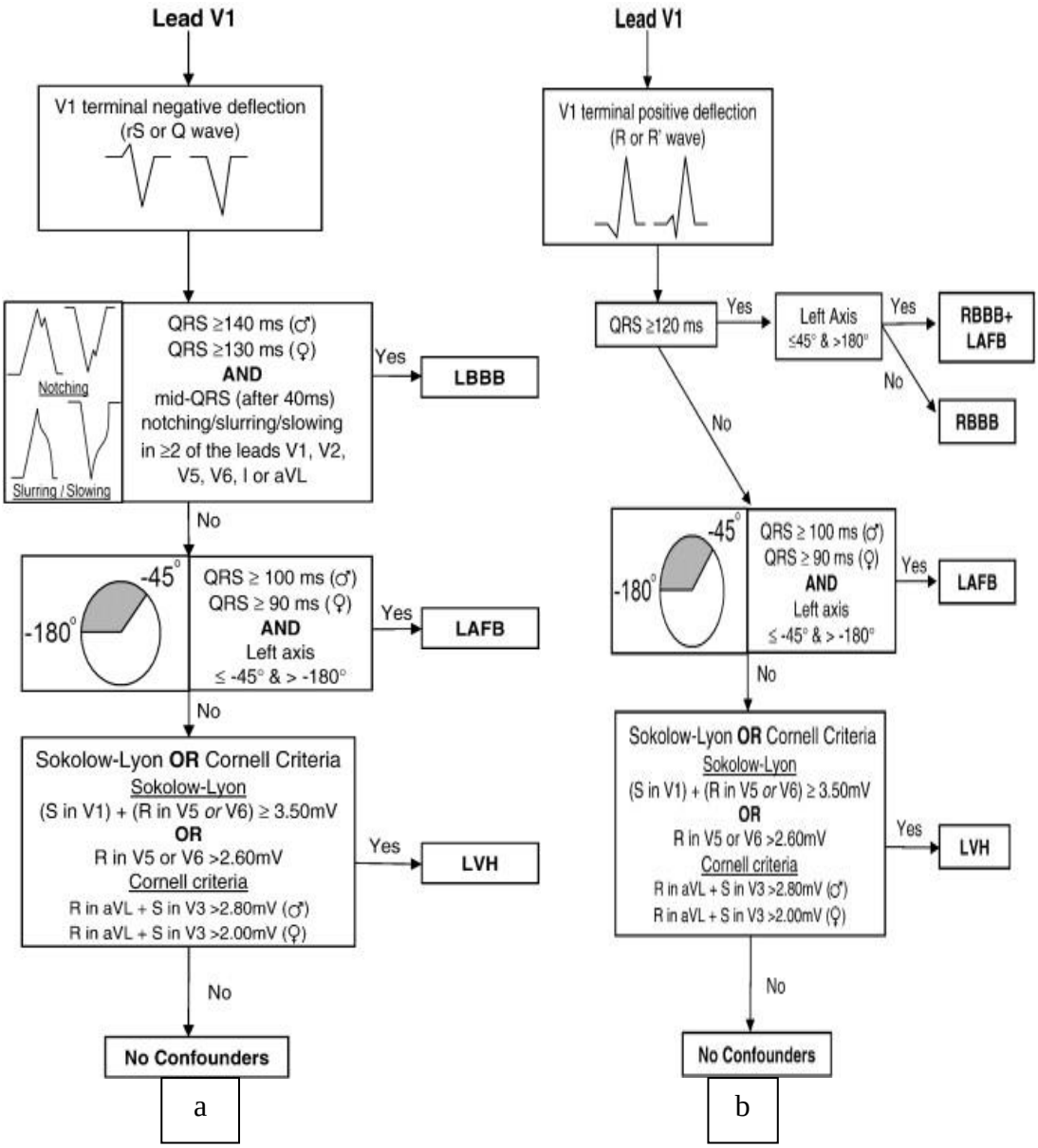

Figure (3-8) A chart that determines the type of conduction when (a) the QRS main wave is downward. (b) the QRS main wave is upward. Where ECG (electrocardiogram), LAFB (left anterior fascicular block), LBBB (left bundle branch block), RBBB (right bundle branch block), (loring *et al*., 2011).

Following that, the P waves in V1 and aVF were examined to determine whether right atrial overload (RAO) was present or not as demonstrated in **Figure (3-9)**. When RAO is present, RVH is often present as well.

Large R waves in V1 and V2 are particular locations indicating posterolateral infarction in the LV or, in the event of LBBB, anteroseptal

infarction, but in the case of RAO large R waves in V1 and V2 are likely caused by RVH rather than infarction.

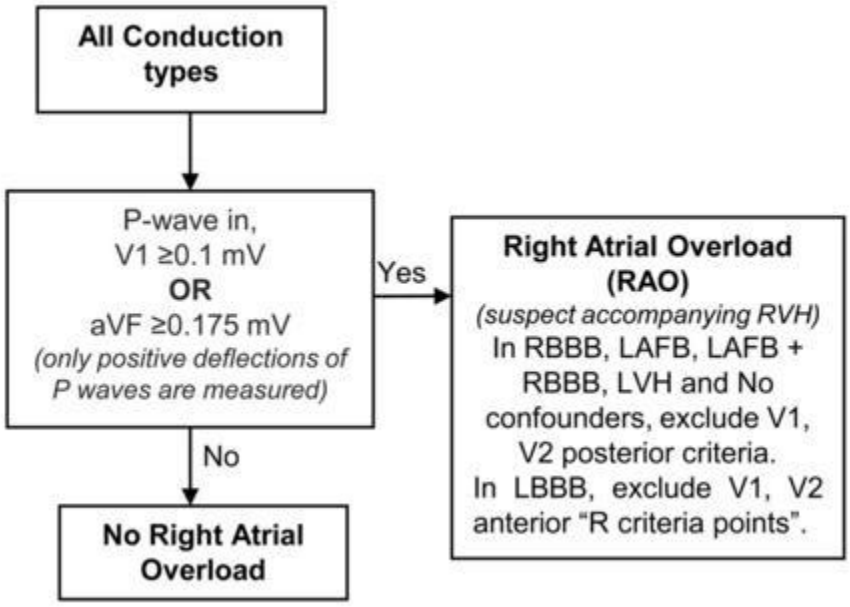

Figure (3-9) A chart for the identification of right atrial overload (RAO).

In the case of LVH, Q waves may be present in leads V1-V3 even without infarction, but the presence of infarction in other leads raises the possibility that the infarction was the source of the Q waves in V1-V3. If the leading I, aVL, V4, V5, or V6 scored 4 or more QRS points, then the Q waves in V1-V3 awarded QRS points.

Then measurements of both amplitudes and durations were done. Weighting and selection were also performed, where the weighting refers to the number of points granted for the criteria satisfied, while selection represents the process of choosing a single criterion from a group, only the first satisfied criterion should be selected in each box, then the QRS score multiplied by 3 to obtain LV infarct size, where LV infarct size = 3 * QRS score, **figure (3-10)**.

Lead	RBBB		LAFB		LAFB+RBBB		LVH		No Confounders	
	Criteria	**Pts**	**Criteria**	**Pts**	**Criteria**	**Pts**	**Criteria**	**Pts**	**Criteria**	**Pts**
I	Q≥30ms	1	Q≥30ms	1	Q≥30ms	1	Q≥30ms	1	Q≥30ms	1
	R/Q≤1 R≤0.2mV	1	R/Q≤1 R≤0.2mV	1	R/Q≤1 R≤0.2mV	1	R/Q≤1 R≤0.2mV	1	R/Q≤1 R≤0.2mV	1
II	Q≥40ms	2	Q≥40ms	2	Q≥40ms	2	Q≥40ms	2	Q≥40ms	2
	Q≥30ms	1	Q≥30ms	1	Q≥30ms	1	Q≥30ms	1	Q≥30ms	1
aVL	Q≥30ms	1	Q≥40ms	1	Q≥40ms	1	Q≥40ms	1	Q≥30ms	1
	R/Q≤1	1	R/Q≤1	1	R/Q≤1	1	R/Q≤1	1	R/Q≤1	1
aVF	Q≥50ms	3	Q≥50ms	3	Q≥50ms	3	Q≥60ms	3	Q≥50ms	3
	Q≥40ms	2	Q≥40ms	2	Q≥40ms	2	Q≥50ms	2	Q≥40ms	2
	Q≥30ms	1	Q≥30ms	1	Q≥30ms	1	Q≥40ms	1	Q≥30ms	1
	R/Q≤1	2	R/Q≤1	2	R/Q≤1	2	R/Q≤1	2	R/Q≤1	2
	R/Q≤2	1	R/Q≤2	1	R/Q≤2	1	R/Q≤2	1	R/Q≤2	1
V1 Ant.	Q≥50ms	2	any QR	1	Q≥50ms	2	any QR		any Q	1
	any Q	1			any Q	1	(or any Q if*)	1		
	Init R≤20ms						NtchInit40			
V1 Post.**			R/S≥1	1			R/S≥1	1	R/S≥1	1
	Init R≥60ms	2	R≥50ms	2	Init R≥60ms	2	R≥50ms	2	R≥50ms	2
	Init R≥ 1.5mV		R≥1mV		Init R≥ 1.5mV		R≥1mV		R≥1mV	
	Init R≥50ms	1	R≥40ms	1	Init R≥50ms	1	R≥40ms	1	R≥40ms	1
	Init R≥1.0mV		R≥0.7mV		Init R≥1.0mV		R≥0.7mV		R≥0.7mV	
			Q≤0.2&S≤0.2mV	1			Q≤0.2&S≤0.2mV	1	Q≤0.2&S≤0.2mV	1
V2 Ant.	Q≥50ms	2			Q≥50ms	2				
	any Q	1	any QR	1	any Q	1	any QR	1	any Q	1
	R≤10ms		R≤10ms		R≤10ms		(or any Q if*)		R≤10ms	
	R≤0.1mV		R≤0.1mV		R≤0.1mV		NtchInit40		R≤0.1mV	
V2 Post.**			R/S≥1.5	1			R/S≥1.5	1	R/S≥1.5	1
	Init R≥70ms	2			Init R≥70ms	2				
	Init R≥2.5mV		R≥60ms	2	Init R≥2.5mV		R≥60ms	2	R≥60ms	2
	Init R≥50ms	1	R≥2mV		Init R≥50ms	1	R≥2mV		R≥2mV	
	Init R≥2.0mV		R≥50ms	1	Init R≥2.0mV		R≥50ms	1	R≥50ms	1
			R≥1.5 mV				R≥1.5 mV		R≥1.5 mV	
			Q≤0.3&S≤0.3mV	1			Q≤0.3&S≤0.3mV	1	Q≤0.3&S≤0.3mV	1
V3	Q≥30ms	2	Q≥30ms	2	Q≥30ms	2	QR&(Q≥30ms)	2	Q≥30ms	2
	R≤10ms		R≤10ms		R≤10ms		NtchInit40	1	R≤10ms	
	Q≥20ms	1	Q≥20ms	1	Q≥20ms	1	any QR		Q≥20ms	1
	R≤20ms		R≤20ms		R≤20ms		(or any Q if*)		R≤20ms	
V4	Q≥20ms	1	Q≥20ms	1	Q≥20ms	1	Q≥20ms	1	Q≥20ms	1
	R/Q≤0.5	2	R/Q≤0.5	2	R/Q≤0.5	2	R/Q≤0.5	2	R/Q≤0.5	2
	R/S≤0.5		R/S≤0.5		R/S≤0.5		R/S≤0.5		R/S≤0.5	
	R/Q≤1	1	R/Q≤1	1	R/Q≤1	1	R/Q≤1	1	R/Q≤1	1
	R/S≤1		R/S≤1		R/S≤1		R/S≤1		R/S≤1	
	R≤0.5mV		R≤0.5mV		R≤0.5mV		R≤0.5mV		R≤0.5mV	
	NtchInit40		NtchInit40		NtchInit40		NtchInit40		NtchInit40	
V5	Q≥30ms	1	Q≥30ms	1	Q≥30ms	1	Q≥30ms	1	Q≥30ms	1
	R/Q≤1	2	R/Q≤1	2	R/Q≤1	2	R/Q≤1	2	R/Q≤1	2
	R/S≤1		R/S≤1		R/S≤1		R/S≤1		R/S≤1	
	R/Q≤2	1	R/Q≤2	1	R/Q≤2	1	R/Q≤2	1	R/Q≤2	1
	R/S≤2		R/S≤1.5		R/S≤1.5		R/S≤2		R/S≤2	
	R≤0.6mV		R≤0.6mV		R≤0.6mV		R≤0.6mV		R≤0.6mV	
	NtchInit40		NtchInit40		NtchInit40		NtchInit40		NtchInit40	
V6	Q≥30ms	1	Q≥30ms	1	Q≥30ms	1	Q≥30ms	1	Q≥30ms	1
	R/Q≤1	2	R/Q≤1	2	R/Q≤1	2	R/Q≤1	2	R/Q≤1	2
	R/S≤1		R/S≤1		R/S≤1		R/S≤1		R/S≤1	
	R/Q≤3	1	R/Q≤3	1	R/Q≤3	1	R/Q≤3	1	R/Q≤3	1
	R/S≤3		R/S≤2		R/S≤2		R/S≤3		R/S≤3	
	R≤0.6mV		R≤0.6mV		R≤0.6mV		R≤0.6mV		R≤0.6mV	
	NtchInit40		NtchInit40		NtchInit40		NtchInit40		NtchInit40	
Total	Points		Points		Points		Points		Points	
	%LV infarct (3*pts)		%LV infarct (3*pts)		%LV infarct (3*pts)		%LV infarct (3*pts)		%LV infarct (3*pts)	

*(for LVH) if≥4 other points in leads I, aVL, V4, V5 or V6 then count QS in V1-V3
**(RAO) if P positive amp in V1≥0.1mV or aVF P≥0.175mV, then exclude V1-V2 Post criteria

(a)

LBBB		
Lead	**Criteria**	**Pts**
I	any Q	1
	R/Q≤1 R/S≤1	2
	R/Q≤1.5 R/S≤1.5	1
II	Q≥40ms	2
	Q≥30ms	1
	R/Q≤0.5 R/S≤0.5	1
aVL	Q≥50ms	2
	Q≥40ms	1
	R/S≤0.5 R/Q≤0.5	2
	R/S≤1 R/Q≤1	1
aVF	Q≥50ms	2
	Q≥40ms	1
	R/Q≤0.5 R/S≤0.5	1
V1 Ant.* **	NtchInit40	1
	R≥0.3mV R≥30ms	2
	R≥0.2mV R≥20ms	1
V1 Post	S/S`≥2.0	3
	S/S`≥1.5	2
	S/S`≥1.25	1
V2 Ant.* **	NtchInit40	1
	R≥0.4mV R≥30ms	2
	R≥0.3mV R≥20ms	1
V2 Post	S/S`≥2.5	3
	S/S`≥2	2
	S/S`≥1. 5	1
V5	any Q	1
	R/R`≥2 R/R`≥1 R/S≤2	2 1
	R≤0.5mV	1
V6	Q≥20ms	1
	R/R`≥2 R/R`≥1 R/S≤2	2 1
	R≤0.6mV	1
Total	Points	

%LV infarct (3*pts)

***(RAO) if P positive amp in V1≥0.1mV or aVF P≥0.175mV, then exclude V1-V2 R-criteria points

(b)

Figure (3-10) The QRS score sheet for measurement of left ventricular infarct size (a) in the presence of RBBB, LAFB, RBBB+LAFB, LVH, no confounders, (b) in the presence of LBBB. Where (NchInit40) represents a reversal of direction more than 90 degrees that occurs within the first 40 milliseconds of the entire QRS complex. While "Init R" (the peak of initial R wave) represents a reversal of direction more than 90 degrees that occurs within the first 50 milliseconds (loring *et al*., 2011).

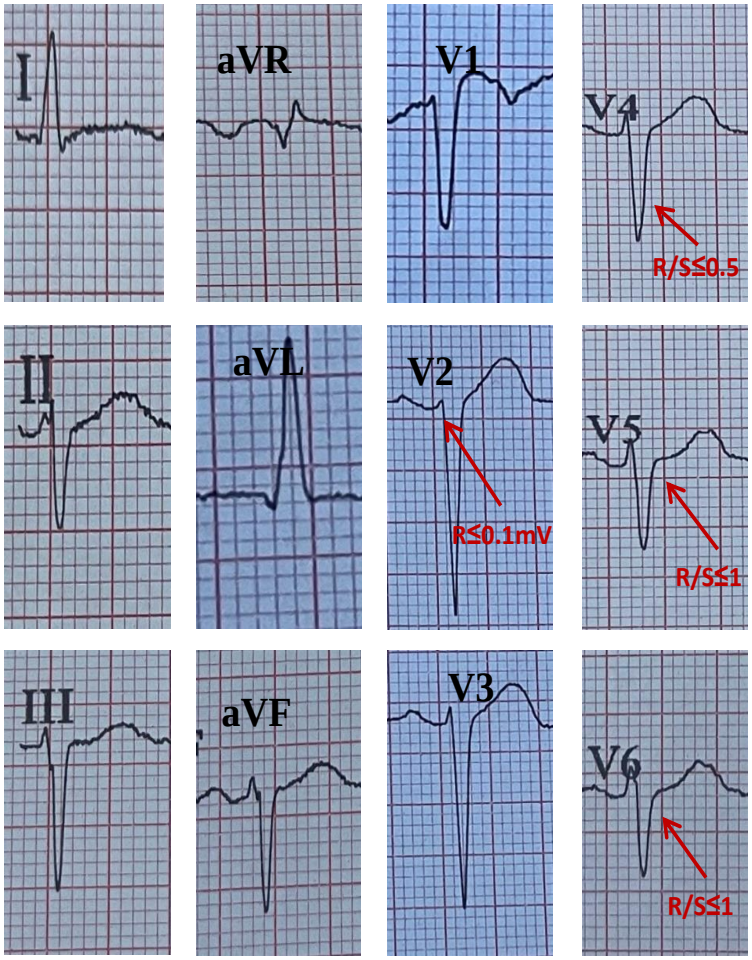

Lead	LAFB Criteria	Pts
I	Q≥30ms	1
	R/Q≤1 R≤0.2mV	1
II	Q≥40ms	2
	Q≥30ms	1
aVL	Q≥40ms	1
	R/Q≤1	1
aVF	Q≥50ms	3
	Q≥40ms	2
	Q≥30ms	1
	R/Q≤1	2
	R/Q≤2	1
V1 Ant.	any QR	1
V1 Post.**	R/S≥1	1
	R≥50ms R≥1mV	2
	R≥40ms R≥0.7mV	1
	Q≤0.2&S≤0.2mV	1
V2 Ant.	any QR	1
	R≤10ms R≤0.1mV	
V2 Post.**	R/S≥1.5	1
	R≥60ms R≥2mV	2
	R≥50ms R≥1.5 mV	1
	Q≤0.3&S≤0.3mV	1
V3	Q≥30ms R≤10ms	2
	Q≥20ms R≤20ms	1
V4	Q≥20ms	1
	R/Q≤0.5 R/S≤0.5	2
	R/Q≤1 R/S≤1 R≤0.5mV NtchInit40	1
V5	Q≥30ms	1
	R/Q≤1 R/S≤1	2
	R/Q≤2 R/S≤1.5 R≤0.6mV NtchInit40	1
V6	Q≥30ms	1
	R/Q≤1 R/S≤1	2
	R/Q≤3 R/S≤2 R≤0.6mV NtchInit40	1
Total	Points	7

LV infarct size= 21

Figure (3-11) Measurement of left ventricular infarct size from Selvestor score.

3.2.4. Statistical analysis

The collected data were analyzed by SPSS-23, and all values were expressed as mean and standard deviation. Continuous variables were compared by using an independent t-test. The relationship between different variables was done by Pearson`s (r) correlation coefficients. Receiver operating characteristic curve (ROC-curve) was used for the assessment of cutoff values for the variables and the sensitivity and specificity percentages.

The probability (P) value <0.05 is considered significant , and highly significant when the p-value <0.001(Khanna *et al*., 2020).

Chapter Four

Results

CHAPTER FOUR

RESULTS

4.1. Demographic data:

This study involved 50 patients with old anterior myocardial infarction with male and female percentages 82.30% and 17.70% respectively **figure (4-1)**, and 50 subjects as the control group (male and female percentages 80.6% and 19.4% respectively). The mean age ± standard deviation (SD) of the patient group is 59.21± 5.597. The percentage of high and normal BMI of the patients is about 82.6%,17.3%, respectively.

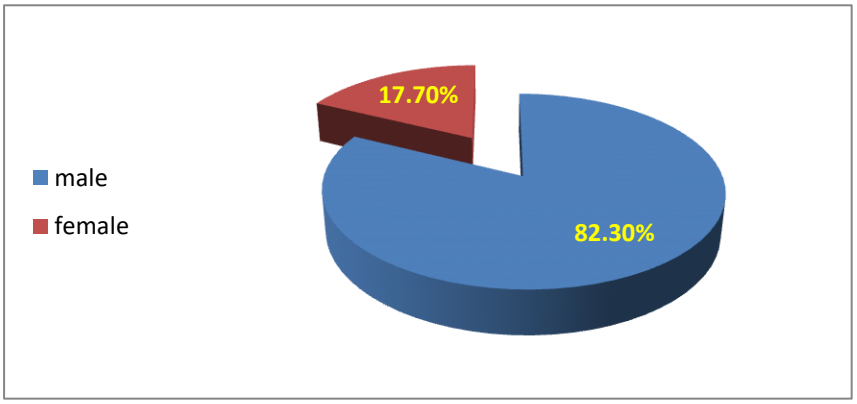

Figure (4-1) Male and female perecntage in patients with old anterior myocardial infarction.

4.2. Comparison between echocardiographic measurements between patients and control groups:

All demographic data, 2D , and 3D echocardiographic measurements are presented in **table (4-1)** and **table (4-2)** as mean ± SD, the probability (P) value < 0.05 considered statistically significant.

Table (4-1) Comparison between the demographic data, axes, and indices measurements in patients and control groups. Values are presented as mean ± standard deviation.

Parameters	Patients group N=50	Control group N=50	P value
Age (year)	59.2±5.597	57.6±7.164	0.212
Weight (Kg)	82.8±12	80.8±13.2	0.436
Height (cm)	170.6±6.9	168.7±9.4	0.269
Body mass index	28.44±4	28.42±4.4	0.983
Body surface area	1.97±0.16	1.94±0.18	0.345
long axis dimension	8.9±0.79	8.34±0.76	0.000**
Short axis dimension	5.17±0.98	4.11±0.51	0.000**
apical dimension	3.54±0.73	2.39±0.41	0.000**
conicity index	0.69±0.12	0.58±0.07	0.000**
Sphericity index (2D)	0.58±0.11	0.49±0.05	0.000**
Sphericity index (3D)	0.38±0.12	0.32±0.06	0.03*
SIv (EDV/1/6*π*L^3)	0.41±0.09	0.33±0.17	0.011*

Where Kg (Kilogram), cm (centimeter), SIv (sphericity index measured by equation),

*P value < 0.05 considered statistically significant.

** P value < 0.000 considered statistically highly significant.

Table (4-2) Comparison between systolic, diastolic, and mitral regurgitation parameters measurements in patients and control groups. Values are presented as mean ± standard deviation.

Parameters	Patients group N=50	Control group N=50	P value
Ejection fraction (2D)	40%±0.09	61%±0.06	0.000**
Ejection fraction (3D)	36%±0.09	60%±0.04	0.000**
EDV (2D)	158.18±63.3	106±26.5	0.000**
EDV (3D)	128.9±54.4	83.4±27.7	0.000**
ESV (2D)	98.36±51.5	42.29±18.7	0.000**
ESV (3D)	85.08±45.44	34.11±11.04	0.000**
Stroke volume (2D)	59.82±19.5	63.03±16.9	0.04*
Stroke volume (3D)	42.96±18.1	52.28±16.3	0.009
E/A	1.46±1.24	1.25±0.37	0.245
E/e'	13.03±7.9	5.82±1.48	0.000**
Left atrial volume index	24.23±15.62	15.98±6.9	0.001*
TR velocity	1.60±1.13	1.24±0.46	0.085
Tenting area of MV	1.45±1.06	0.61±0.16	0.000**
Cooptation distance MV	0.79±0.22	0.56±0.13	0.000**

Where EDV (end diastolic volume), ESV (end systolic volume), TR (tricuspid regurgitation), MV (mitral valve).

*P value < 0.05 considered statistically significant

** P value < 0.000 considered statistically highly significant.

There were statistically non-significant differences regarding the age ,BSA and BMI between the patients and control groups (p = 0.212, 0.345, and 0.983 respectively).

2D, 3D echocardiographic parameters : long axis, short axis and apical dimensions, indices : conicity, sphericity indices (CI, SI), and SI measured by equation (SIv), LV volumes : end diastolic volume (EDV) and end systolic volume (ESV) of patients group were statistically higher than those of the control group (p< 0.000).

2D, 3D echocardiographically derived ejection fractions (EF) were statistically lower in the patient group than the control group, with high significance (p<0.000). Stroke volume (SV) was statistically lower in the patients group than the control group (p=0.04 for 2D echocardiographic derived SV and p<0.000 for 3D derived SV).

Assessment of left ventricular diastolic function depending on E/A ratio, E/e′, LA volume index, and TR velocity revealed the presence of 76.90% of the patients with left ventricular diastolic dysfunction (LVDD) grade 1, and 23.1% of LVDD grade 2-3, **figure (4-2)**.

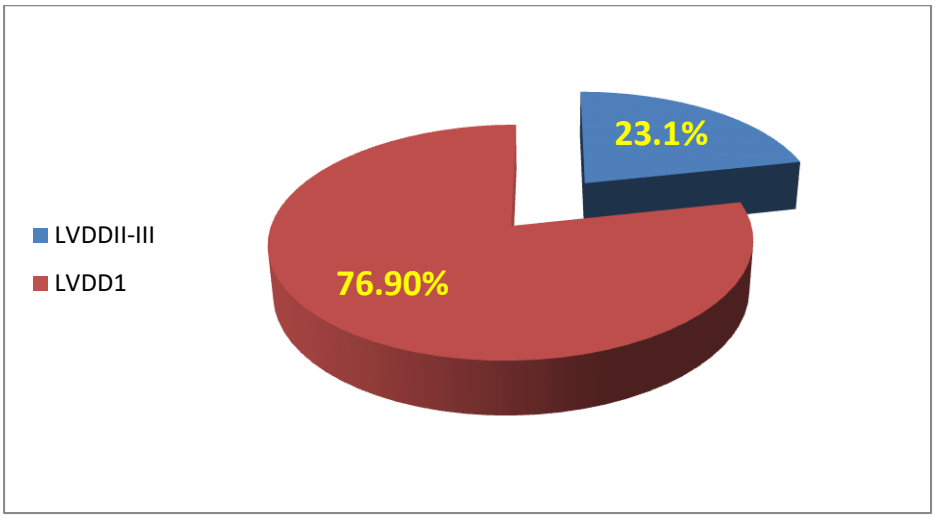

Figure (4-2) Percentage of left ventricular diastolic dysfunction grade1 (LVDDI) and grade 2-3 (LVDDII-III).

E/A ratio and TR velocity in patients group were higher than control group but statistically non-significant ($p>0.05$), LA volume index was larger than control group with statistically high significance ($p=0.001$). There was highly significant difference regarding the E/e´ between the two groups ($p<0.000$).

4.3. Comparison between 2D and 3D echo derived parameters:

2D-echocardiographically derived SI was higher than 3D-SI and SIv with high statistical significance ($p=0.000$), but there was no statistical difference between 3D-SI and SIv ($p=0.224$). There were statistically significant differences regarding 2D, 3D-EF, and SV with values of 2D being higher than 3D measures ($p=0.026$, 0.000, respectively), **figure (4-3).** 2D-EDV value was higher than 3D-EDV with statistical significance ($p =0.008$). 2D-ESV was higher than 3D-ESV but statistically not significant ($p=0.113$), **figure** (**4-3)**.

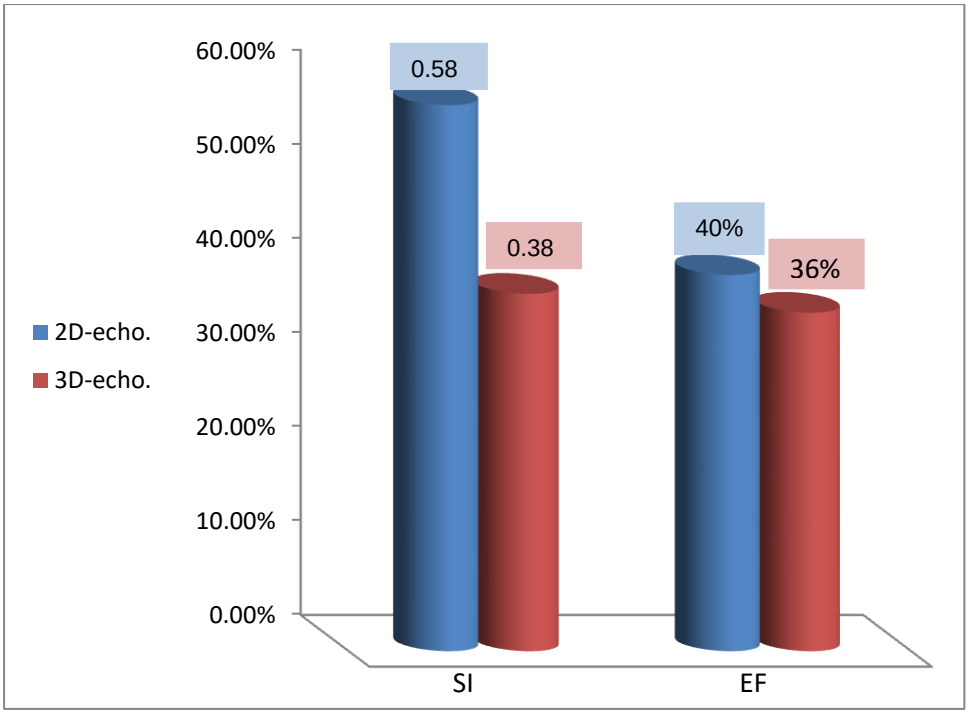

(a)

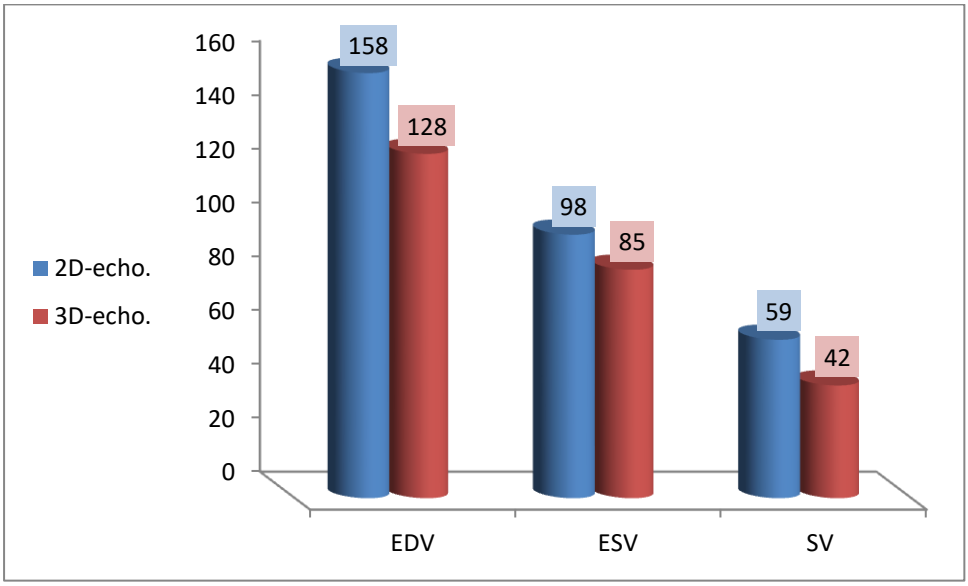

(b)

Figure (4-3) (a) Comparison between 2D and 3D echocardiographic derived sphericity index (SI), ejection fraction (EF). **(b)** Comparison between 2D and 3D echocardiographic derived end diastolic volume (EDV), end systolic volume (ESV), and stroke volume (SV).

4.4. Correlation studies between different echocardiographic parameters:

Correlation studies were done in patients group, between CI, 2D and 3D echo derived SI with different LV systolic, diastolic parameters, and MR related measurements, as demonstrated in, **table (4-3)**.

Table (4-3) Correlation studies between 2D, 3D echocardiographically derived sphericity index and conicity with different echocardiographic parameters.

Parameters	Conicity index		Sphericity index(2D)		Sphericity index(3D)	
	r	P	r	P	r	P
EF (2D)	-0.100	0.486	-0.524**	0.000	-0.419**	0.002
EF (3D)	-0.095	0.505	-0.414**	0.003	-0.475**	0.000
EDV (2D)	-0.135	0.350	0.629**	0.000	0.512**	0.000
EDV (3D)	-0.181	0.207	0.398**	0.004	0.523**	0.000
ESV (2D)	-0.131	0.365	0.667**	0.000	0.527**	0.000
ESV (3D)	-0.177	0.220	0.469**	0.001	0.573**	0.000
SV (2D)	-0.182	0.205	-0.350*	0.025	-0.478	0.023
SV (3D)	-0.092	0.524	-0.41	0.020	-0.557	0.010
E/A	0.142	0.320	0.053	0.713	0.139	0.335
E/e'	0.149	0.35	0.18	0.251	0.246	0.120
LAVI	0.20	0.21	0.33*	0.035	0.3*	0.049
TR velocity	0.067	0.668	0.149	0.340	0.035	0.827
Tentening area of MV	0.042	0.773	0.257	0.072	0.296*	0.045
cooptation distance MV	0.052	0.718	0.453**	0.001	0.652**	0.000
VC of MR	0.186	0.251	0.346*	0.027	0.525**	0.001

Where EF (ejection fraction), EDV (end diastolic volume), ESV (end systolic volume), SV (stroke volume), LAVI (left atrial volume index), TR (tricuspid regurgitation), MV (mitral valve), VC (vena contracta), MR (mitral regurgitation).

** Correlation is highly significant at the 0.01 level (2-tailed), * Correlation is significant at the 0.05 level (2-tailed).

The conicity index showed a statistically non significant negative correlation with 2D, 3D derived EF and SV (P>0.05), while SI showed a highly statistically significant negative correlation with EF, for 2D, 3D-SI with 2D, 3D-EF (P<0.01), and statistically significant negative correlation with SV, for 2D, 3D-SI with 2D, 3D-SV (P<0.05).

There was a negative correlation of CI with EDV and ESV (2D and 3D echo derived) but it was statistically not significant (P>0.05). On the other side, these correlation studies show a highly significant positive correlation of SI with EDV and ESV (P<0.000).

Regarding the correlation studies of CI and SI with LV diastolic parameters (E/A, E/e' and TR velocity) showed positive correlation but statistically non-significant (P>0.05), CI also showed non significant positive correlation with LAVI (P>0.05), but there was significant positive correlation of 2D, 3D-SI with LAVI (P<0.05), as demonstrated in **table (4-2)**.

4.5. Mitral regurgitation:

Secondary MR presented in 65.4% of the patients ranging from mild MR (70.6%) and moderate MR (29.4%), **figure (4-4)**. In the patients, the mean of vena contracta (VC) was 0.25±0.16. The control group showed only trace MR if present, so no comparison was done between the vena contracta of the two groups.

Tenting area of MV and cooptation distance of MV showed statistically highly significant differences between the patients and control groups (p <0.000).

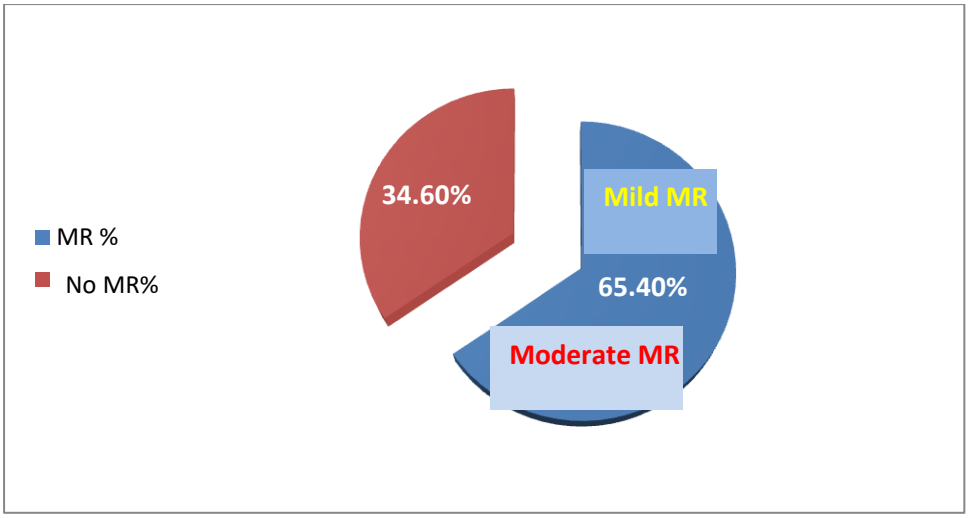

Figure (4-4) Percentage of mitral regurgitation (MR) in patients group.

There was statistically non significant correlation between CI with MR parameters (VC, tenting area, and cooptation distance), (P>0.05).

2D, 3D-SI showed positive correlations with MR parameters (VC of MR, MV tenting area and cooptation distance), and especially 3D-SI was more significant with VC than 2D-SI , (P values for 2D-SI: 0.027, 0.072, 0.001 respectively; 3D-SI: 0.001, 0.045, 0.000 respectively), **table (4-3)**.

Patients with moderate MR showed higher 2D, 3D–SI (0.62 ± 0.14, 0.49±0.18, respectively) than patients with mild MR (0.57 ± 0.107, 0.35 ± 0.08) with statistically non significance difference for 2D-SI with MR (p=0.24), and statistically highly significant difference for 3D-SI with MR (p=0.001). There was no statistical difference between CI in mild and moderate MR (CI in mild MR 0.7±0.12, in moderate MR 0.67 ± 0.13,P= 0.624), **figure (4-5)**.

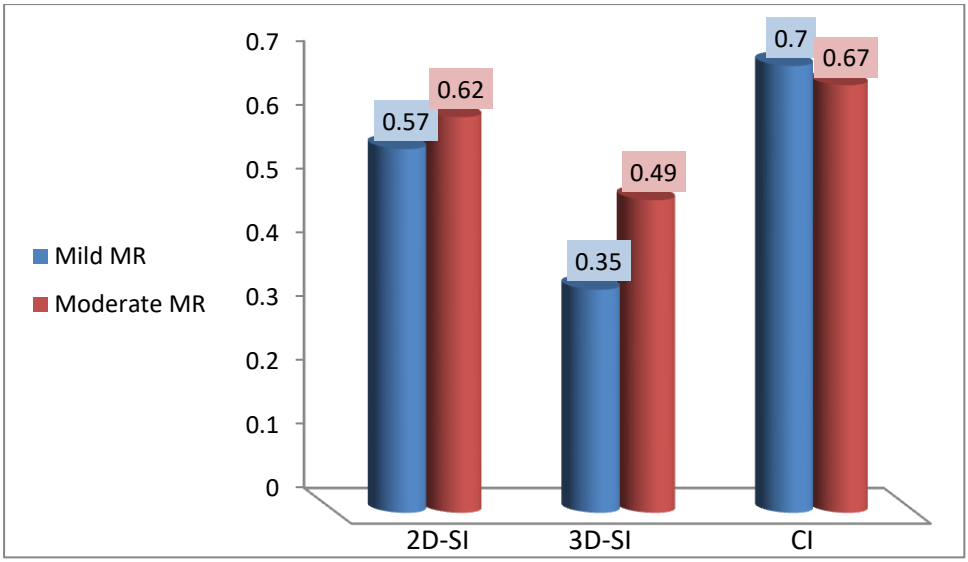

Figure (4-5) Comparison between echocardiographic derived sphericity, conicity index (2D,3D-SI, and CI) in patients with mild and moderate mitral regurgitation (MR).

4.6. Selvester QRS score:

The Selvester QRS scores of all patients were distributed from 1 to 15 points, with a mean of 6.1 ±3.51 points and accordingly LV infarct size ranged from 3%-45%, with mean of 20%±0.093**.**

Correlation studies of LV infarct size with LV remodelling indices (CI, 2D and 3D-SI) showed no significant correlation with CI (p=0.929), **figure (4-6)**, there were positive correlation but statistically non-significant with 2D-SI, and statistically significant with 3D-SI (P=0.377, 0.044 ,respectively), as seen in **figure (4-7)**.

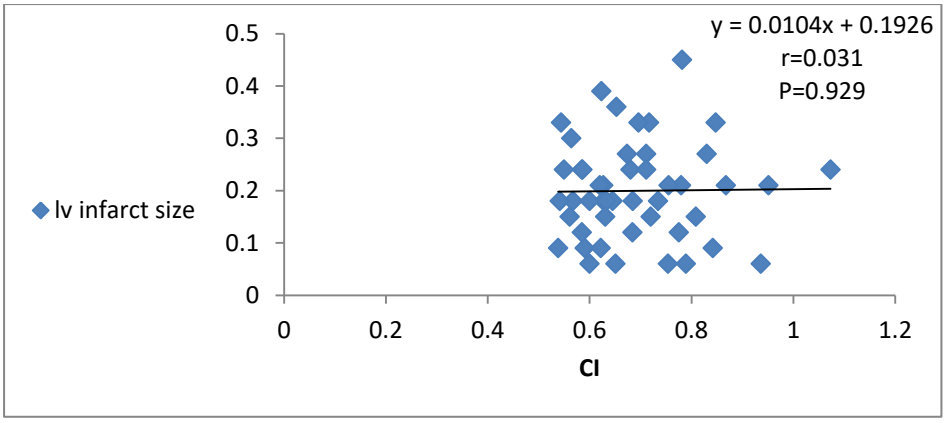

Figure (4-6) Correlation studies of Selvester QRS score derived left ventricular infarct size with echocardiographic derived conicity index (CI).

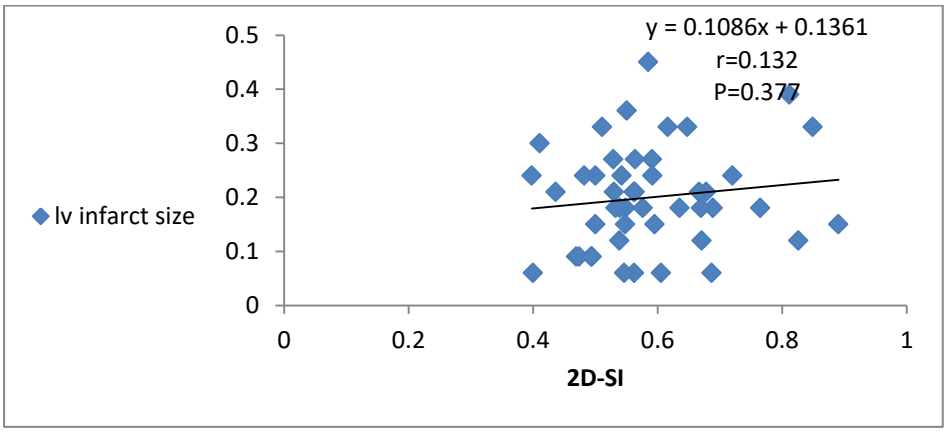

(a)

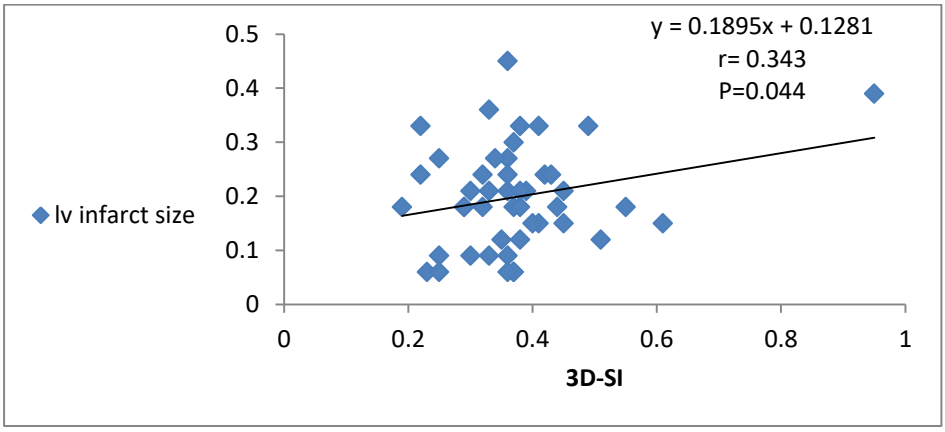

(b)

Figure (4-7) Correlation studies between infarct size of left ventricle by Selvester score with (a) 2D sphericity indices (2D-SI), (b) 3D sphericity indices (3D-SI).

Correlation studies of LV infarct size with LV diastolic and systolic parameters revealed statistically significant positive correlation with E/e′ (p=0.004), as shown in **figure (4-8)**, and statistically significant negative correlation with 2,3D-EF (p= 0.004, 0.000, respectively), **figure (4-9)**.

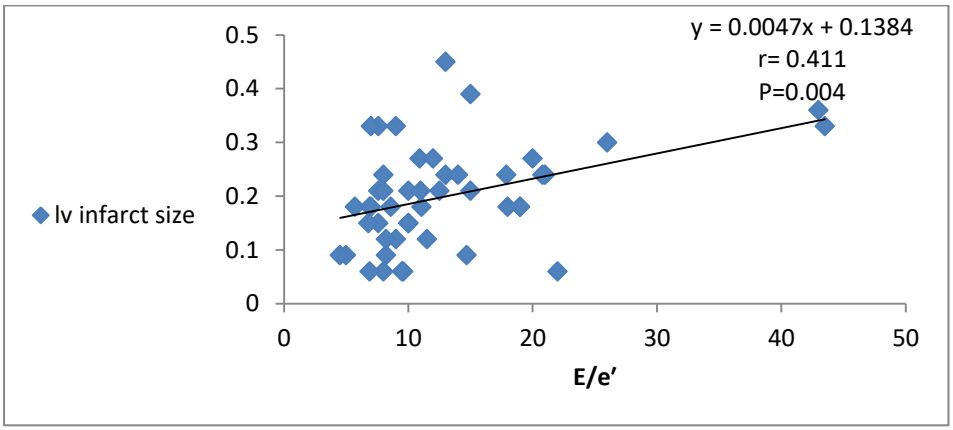

Figure (4-8) Correlation studies between left ventricular infarct size by selvester score with echocardiographic derived E/e′ of mitral valve inflow.

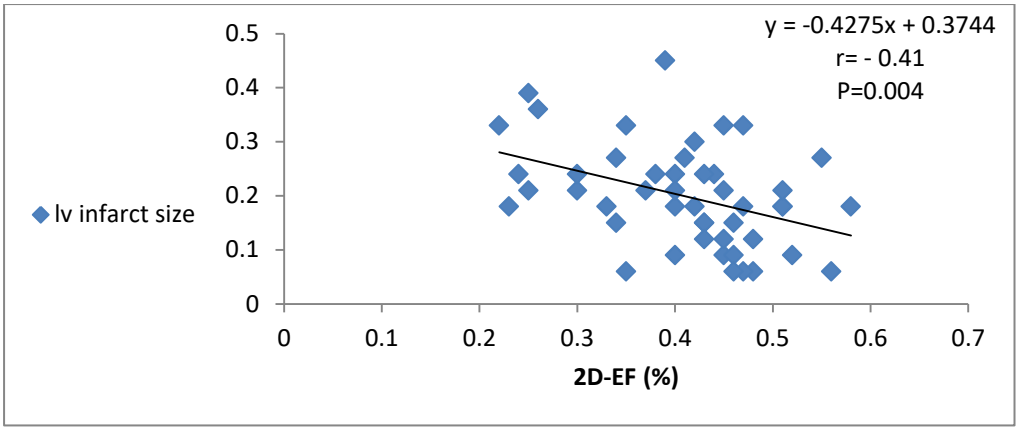

(a)

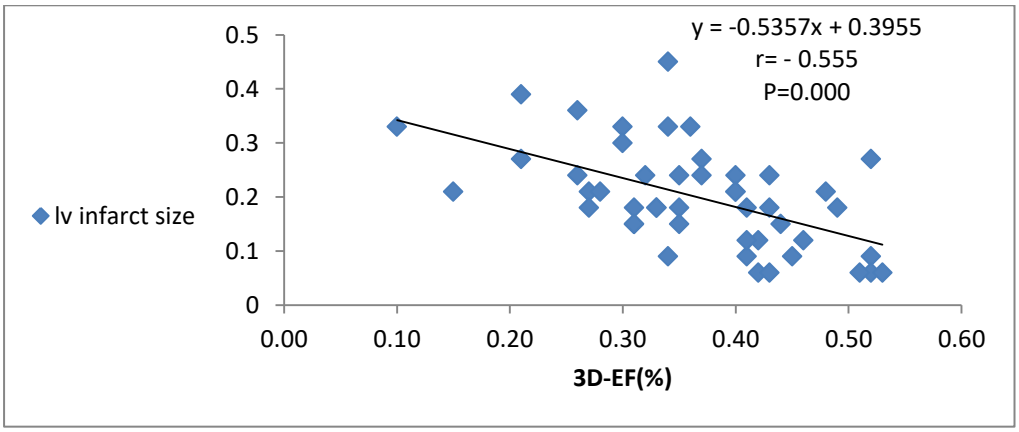

(b)

Figure (4-9) Correlation studies between left ventricular infarct size by selvester score, and (a) 2D echocardiographic derives ejection fraction (2D-EF) and (b) 3D ejection fraction (3D-EF).

4.7. Receiver operating characteristic sensitivity and specificity for LV remodelling indices:

The area under the curve (AUC) for 3D-SI was 0.929 with sensitivity of 83% and specificity of 82% for a cutoff value of 0.33, **figure (4-10)**.

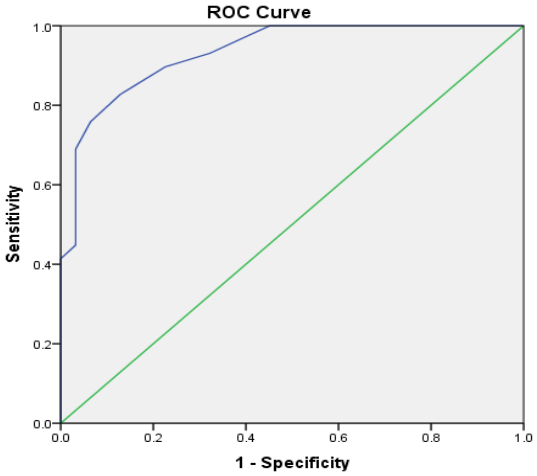

Figure (4-10) Receiver operating characteristic for 3D sphericity index.

The area under the curve (AUC) for 2D-SI was 0.75 with sensitivity 74% and specificity of 70% for a cutoff value of 0.53, **figure (4-11).**

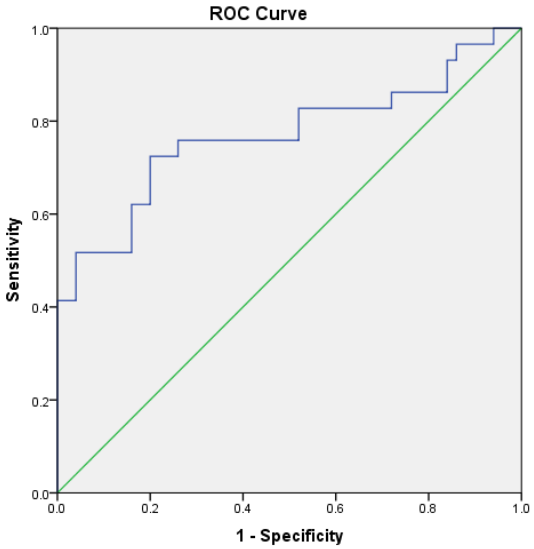

Figure (4-11) Receiver operating characteristic for 2D sphericity index.

The area under the curve (AUC) for CI was 0.78 with sensitivity 71% and specificity of 74% for a cutoff value of 0.62, **figure (4-12).**

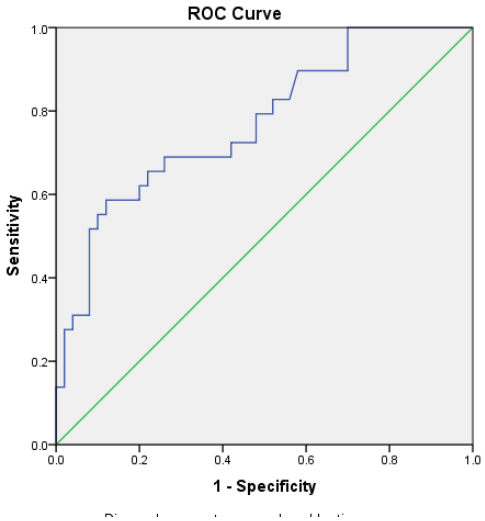

Figure (4-12) Receiver operating characteristic for conicity index.

Chapter five

Discussion

CHAPTER FIVE

DISCUSSION

5.1. Demographic data:

5.1.1. Effect of sex:

This study showed a higher prevalence rate in males in comparison to females in MI patients, and this matches results in other studies (Mohseni *et al*., 2017; Sharif & Lafi, 2021). Christensen *et al*. (2022) also demonstrated that the prevalence of MI was higher among males.

A study conducted by Albrektsen and his colleagues to determine the risk of incident of MI in males and females, the study showed that males have twice the risk of MI in comparison with females. The risk in both sex increases with age, but females are at the least risk (Albrektsen *et al*., 2016). The low risk of MI in premenopausal women is due to the beneficial effect of estrogen on decreasing LDL and increasing HDL and its effect on the blood vessels (Coutinho, 2014).

An opposite to another study that found an absence of the relationship between menopause and atherosclerosis (Wolff *et al*., 2013).

5.1.2. Effect of age:

In this study, the mean age of the patients with MI was 59.21, which is close to other studies that suggested the mean age of MI was 58.4, 62.1, and 58.13 years (Duraes *et al*., 2017; Khanna *et al*., 2020; Kaplangoray *et al*., 2023) respectively.

The mean age of MI patients was 55.5 years, ranging from 20–90 years. The highest prevalence rate of MI was noticed in older patients 33.8% in the age group of 60–69 years and 28.4% at 50–59 years (Amen *et al*., 2020).

Herrett *et al*. (2015) demonstrated that the incidence of MI ranges from 0.06% of men <45 years of age to 2.46% of those ≥75 years old.

5.1.3. Effect of body mass index:

The mean BMI in this study was 28.44, which is higher than the normal value of 18.5–24.9 kg/m² (Caballero, 2019), and in comparison to other studies found the mean BMI of patients with MI was 26.8, 29.1, 26.7, and 26.3 (Duraes *et al*., 2017; khanna *et al*., 2020; Kaplangoray *et al*., 2023; El-Naggar *et al*., 2023) respectively.

In a study conducted in Erbil by Amen and his co-workers, they demonstrated a high incidence of obesity and overweight among patients with AMI, where 40.55% were overweight, 35.1% were obese, and 24.3% had a normal BMI (Amen *et al*., 2020).

The prevalence of obesity was 75.15% in MI patients, normal BMI was 24.8%. Within ten years after the heart attack, obese patients are most likely to die from heart disease (Sharif & Lafi, 2021).

5.2. The difference in the parameter between patients and control:

On comparison between patients and controls which was matching age, weight, and height.

The study showed a statistically significant increase in 2D and 3D parameters: long, short, and apical axis, conicity and sphericity indices, end diastolic volume and end systolic volume in the patient group than in

control group, this reflects the LV remodelling that alters ventricular size and geometry represented by larger volumes, bigger long and short axis. Also, anterior MI causes dilatation in the apical area of the left ventricle that leads to an increase in the apical axis.

This study concurs well with a study conducted by Di Donato *et al*. (2006) to evaluate LV geometry by sphericity and conicity indices in normal and anterior ischemic cardiomyopathy patients and they found that the long, short, apical axis, CI, SI, EDV, and ESV were higher in the patient group than in control group.

Fan *et al*. (2010) showed that the long, short, apical axis, apical conicity ratio, EDV index, and ESV index by CMR were significantly different in patients with MI than in healthy controls.

In a study conducted by Li *et al*. (2008) to predict LV remodelling after MI, 2D, 3D-SI, and LV volumes were higher in patients than in controls.

Karuzas *et al*. (2019) also found that 3D-SI, EDV, and ESV were higher in patients with LV remodelling than in patients without LV remodelling, this happens due to LV remodelling that occurs after MI as a consequence of sudden overloading of the heart, leading to a serial of changes that involve infarcted and non infarcted tissue, resulting in increased LV volume.

The study showed that 2D, 3D echocardiographically derived ejection fraction and stroke volume were statistically significantly lower in the patient's group than the control group, this could be because, following LV remodelling the myocardium loses its contractile function which leads to a reduction in systolic function.

This is in agreement with a study conducted by Fan and his colleagues to assess LV apical geometry after MI, they demonstrated that EF, SV were lower in patients than in control groups. A normal conic LV apical shape is important for cardiac pump function. Following ischemic injury, the helical apex of the myocardium loosens, causing a spherical myocardial configuration, the oblique apical loop fibers are realigned to a more transverse orientation, resembling the basal loop. These changes lead to reduced LVEF (Fan *et al*., 2010).

Recent study also documented that the EF in patients with ischemic cardiomyopathy was lower in patients than in controls (Emara *et al*., 2021).

Other studies revealed that in patients with LV remodelling, the EF was lower than in patients without remodelling (Vieira *et al*., 2013; Ola *et al*., 2018; Karuzas *et al*., 2019).

E/A ratio and TR velocity in the patient's group were higher than the control group but statistically non-significant, the reason for that could be that in this study, the percentage of moderate mitral regurgitation was 29.4% which lead to increase the E velocity. TR velocity higher in patients than control group could be explained by post capillary changes due to LV diastolic dysfunction which may be later on progress in to post capillary pulmonary hypertension.

LA volume index and E/e´ ratio were larger than the control group with statistically high significance, this could occur as a result of the diastolic function representing the amount of distensibility, in the case of MI, necrotic tissue is substituted by fibrosis which leads to decreased distensibility and so increases the LV filling pressure.

Studies showed there was a statistically significant increase in E/A, E/e′, and LA volume in patients with MI compared to controls (Dogan *et al*., 2013; Emara *et al*., 2021).

E, A, and e' are sensitive to myocardial ischemia, changes in ventricular compliance, preload, and afterload. E/e' represents LV-filling pressure. Diastolic dysfunction occurs when elevated filling pressures are required to maintain normal LV filling in order to preserve stroke volume and cardiac output, elevated LV filling pressures lead to increased LA volume (Dogan *et al*., 2013; Søholm *et al*., 2016).

Tenting area of MV and cooptation distance of MV showed statistically highly significant differences between the patients and control groups, and this is due to LV remodelling and tethering of MV leaflets. This is similar to (Di Donato *et al*., 2006; Avila-Vanzzini *et al*., 2018).

5.3. Comparison between 2D and 3D echocardiographic measurements in patients group:

In this study, 2D-SI was higher than 3D-SI and SIv calculated with a high statistical significance, this could be due to geometric assumptions to which 2DE is subjected in measuring the volumes. But there was no statistical difference between 3D-SI and SIv as the latter depends on theoretical volume not dimensions alone.

This is consistent with other studies (Di Donato *et al*., 2006; Li *et al*., 2008) in which the sphericity index was measured by equation depending on theoretical volume, and by 2DE in patients with MI, the studies showed that the value of SI by 2DE was higher than that, measured by equation.

In some studies, the value of SIv was 0.36, 0.37, and 0.38 in patients with LV remodelling which was closer to our SIv results, which was 0.41, and also closer to 3D-SI in this study, which was 0.38 in patients, Consequently, it reveals how closely values for 3D-SI and SIv are related. (Di Donato *et al*., 2006; Li *et al*., 2008; Karuzas *et al*., 2019) respectively.

In this study, 2D-EF, SV, and EDV were statistically significant higher than 3DE, while 2D-ESV was higher than 3D-ESV but statistically not significant. Left ventricular volumes by 3DE, underestimate EDV and ESV. As with 2DE, this could be due to inclusion of LV trabeculae and papillary muscles within the cavity (Armstrong & Ryan, 2019).

This fits with (Vieira *et al*., 2013) who showed 2D-ESV, EDV were higher than those measured by 3DE.

This finding has not matched previous research that demonstrated that EDV and ESV measured by 3DE were higher than those measured by 2DE (Karuzas *et al*., 2019).

Fukuda *et al*. (2012) demonstrated that LV volumes were similar between 3DE and 2DE.

Recent studies done by (Rodríguez-Zanella *et al*., 2019; Baldea *et al*., 2021) showed the EF was smaller in 3DE than in 2DE, but LV volumes were larger in 3DE than in 2DE. Rodríguez-Zanella *et al*. (2019) explained that the measurement of LV volumes by 2DE is subjected to geometric assumptions on LV shape and is often vulnerable to the foreshortening of the apical views during acquisition.

In a study conducted on a normal person, the LVEF and stroke volume were statistically smaller with 3DE than with 2DE, but LVVs were larger

in 3DE than with 2DE, and also attributed the reason for this to geometric assumptions and foreshortening in 2DE (Muraru *et al*., 2013).

5.4. Correlation studies between between conicity index, 2D and 3D echo derived sphericity index with different echocardiographic parameters

5.4.1. Correlation between sphericity index and conicity index with left ventricular systolic function:

SI showed a highly significant positive correlation with EDV and ESV and a statistically significant negative correlation with EF and SV, this is due to LV remodelling leading to an increase in LV volumes, while a decrease in EF results from systolic dysfunction resulting from a decrease in contractility.

This result correlates favorably with Wong *et al*. (2004) who found impaired LV function with increased sphericity owing to depressed contractility, and the sphericity index is an independent predictor of a decrease in survival rate at 10 years.

Also, it was similar to Tani *et al*. (2005). Studies were done by MRI, which showed that the SI was positively correlated with end diastolic, and end systolic LV volume and inversely correlated with LVEF (Nakamori *et al*., 2017, Halima & Zidi, 2018).

Another study has shown that SI by 3DE is negatively correlated with EF, and positively correlated with LV volumes (Maffessanti *et al*., 2009).

Conicity index showed a statistically non significant negative correlation with 2D, 3D-derived EF, and SV, this finding occurs as a result of the

fact that contraction of mid-papillary area of the LV is responsible for about two-thirds of the LV stroke volume. Also, in normal people, there is a variation in the degree of endocardial excursion and myocardial thickening which is lessened at the apex when compared with the base (Lancellotti *et al*., 2017; Armstrong & Ryan, 2019).

Also CI showed a statistically non significant negative correlation with 2D, 3D-EDV, and ESV, this could be explained by the fact that the CI represents the ratio between the apical axis to the short axis of LV, whenever LV volumes are dilated, the short axis is affected more than the apical resulting in a decrease in CI.

Up to our knowledge no other studies correlate the CI with EDV or ESV, but the results of this study indirectly matched the same results from the tables presented in previous studies that showed that the conicity index was inversely correlated with EDV and ESV (Di Donato *et al*., 2006; Garatti *et al*., 2015).

5.4.2. Correlation between sphericity index and conicity index with left ventricular diastolic function:

The correlation studies of CI and SI with LV diastolic parameters (E/A, E/e', LAVI, and TR velocity) showed a positive correlation. Up to our knowledge, no other previous studies have examined the correlation between sphericity and conicity index with diastolic function.

Previous studies assessed the effect of LV diastolic function and LV remodelling, Silveira and his colleagues (2021) studied echocardiographic predictors of LV remodelling following anterior MI, taking EDV and ESV as parameter of LV remodelling and they found a higher E/E' ratio was observed in the group with LV remodelling, and

within 6 months, an E/E' ratio of 11.56 presented good specificity and sensitivity in forecasting ventricular remodelling.

Flachskampf (2010) stated that E/e' was the only independent predictor of remodelling, in patients at risk for remodelling, left ventricular diastolic pressures are already elevated shortly after infarction, signaling that the diastolic pressure-volume relationship of the left ventricle has changed in response to ischemic injury.

Adhyapak *et al*. (2022) took the relative wall thickness (RWT) as an index of LV remodelling and explained its correlation with diastolic and systolic function in patients with IHD. They explained LV remodelling effect on LV diastolic function as LV remodelling after MI can make the LV wall less distensible with elevated stress on the thinner LV wall, which provokes pressure and volume overload on non-infarcted LV regions and triggers myocardial interstitial fibrosis that results in more deterioration of diastolic dysfunction.

In this study, 2D, 3D-SI showed positive correlations with MR parameters (VC of MR, MV tenting area, and cooptation distance). This is closer to (Di Donato *et al*., 2006; Sadeghpour *et al*., 2008). But there was no significant correlation between CI with MR parameters. This is similar to (Di Donato *et al*., 2006).

In this study, the patients with moderate MR showed higher 2D and 3D-SI than patients with mild MR, with a higher statistical significance for 3D-SI with MR, this is because a higher sphericity index as a result of global LV dilatation causes annular dilatation, leaflet tethering, and displacement of mitral valve leaflets that leads to a decrease in the

competence of the mitral valve, so whenever the increase in the sphericity index is greater, more MR occurs (Garatti *et al*., 2015).

This study is consistent with a previous result by Maffessanti *et al*. (2014) that found the 3D sphericity index in patients with moderate MR was statistically significant higher than that in patients with mild MR. Other studies found that there was a statistically significant correlation between the 2D sphericity index and the degree of MR (Sadeghpour *et al*., 2008; Garatti *et al*., 2015).

The contradictory study proposed that the sphericity index had a poor correlation with MR (Yiu *et al*., 2000).

This study showed no statistical difference between CI in mild and moderate MR, this might be due to the conicity index representing regional shape abnormalities that couldn't affect the mitral valve.

This is in good agreement with Di Donato *et al*. (2006) who explain it as follows in the case of a high conicity index, the apex is dilated with the short axis remaining unchanged, thus the mitral function is better. Garatti *et al*. (2015) also revealed no correlation between CI and the degree of MR.

5.4.3. Correlation between left ventricular infarct size with different parameter:

In this study, we used the Selvester score in calculating the infarct size, as the increase in the Selvester score is directly associated with the increase in the quantity of myocardial scar tissue (Loring *et al*., 2011).

As documented previously, CMR is the gold standard for assessing viability, and the evaluation of scar extent and size using CMR is precise and reproducible (Enein *et al*., 2020). Another study has shown a good correlation between the Selvester score and MRI in determining infarct size (Holmes *et al*., 2016). Thus, this could reflect the applicability of the Selvester score in reflecting infarct size.

This study showed that the mean of the selvester QRS scores of all patients was 6.1 points, suggesting that the QRS score in MI was distributed within a relatively medium-score index. This concurs well with (Holmes *et al*., 2016) who investigated the benefit of the Selvester score in the scoring system in assessing infarct size in patients with MI at both the acute and follow-up periods. Selvester infarct size was 12.98% in patients with anterior MI after 2 months, this means that the Selvester score point was 4.19, which was included in the medium score too.

This classification is according to a previous study done by Tjandrawidjaja *et al*. (2010) that categorized the infarct size, which was estimated from the selvester score, into small infarcts if the selvester score was $\leq$ 3, medium infarcts if the score was 4 to 7, and large infarcts if the score was $\geq$ 8.

5.4.3.1. Correlation between left ventricular infarct size with sphericity index and conicity index:

This study showed no significant correlation between LV infarct size with CI and there was a statistically non-significant positive correlation with 2D-SI but a statistically significant correlation with 3D-SI.

Patients with anterior MI experienced a larger infarction due to more at-risk myocardium, as well as more substantial post-infarction remodelling

and dysfunction (Masci *et al*., 2011). Scar size had a strong linear relationship with LV end-diastolic and end-systolic volumes as LV remodelling parameters (Ørn *et al*., 2007).

Pezel *et al*. (2020) demonstrated that there was no significant relationship between sphericity and conicity indices with LV infarct size by MRI.

In contrast to a study done by Fan *et al*. (2010) by MRI in the population of patients with IHD, the apical conicity ratio demonstrated a significant correlation with scar score.

5.4.3.2. Correlation between left ventricular infarct size with left ventricular diastolic and systolic function:

In this study, there was a statistically significant positive correlation with E/e′ and a statistically significant negative correlation with 2,3D-EF. This might be due to the fact that following MI there was impaired relaxation and stiffness that resulted from collagen accumulation in tissue that altered the elasticity of the myocardium, Whenever the infarct size is enlarged, more diastolic and systolic impairment results.

This supports the previous findings by Kaplangoray *et al*. (2023) that studied the correlation between Selvester score and myocardial performance index, as parameters for systolic and diastolic functions of the heart in patients with acute anterior MI. The study revealed that both tissue Doppler and conventional myocardial performance index were more impaired in patients with a high Selvester score, and there was a strong correlation between Selvester score and myocardial performance index.

Søholm *et al*. (2016) revealed that after STEMI, diastolic dysfunction, as a result of increased LV filling pressure, and systolic dysfunction had a statistically significant correlation with large infarct size. And demonstrate that the systolic dysfunction after MI is linked with a large area of myocardial edema and necrosis that lead to the greater myocardial infarct area.

Also, it is in line with the finding of Behairy and his co-workers (2014), who showed a significant positive correlation between the degree of diastolic dysfunction and the extent of myocardial scarring by CMR in patients with IHD.

In contrast, Chung *et al*. (2014); Sundqvist *et al*. (2022) identified that the degree of myocardial scarring was weakly or not significantly correlated with LV diastolic function. Chung *et al*. (2014) explained this by saying that hypercontractility in the non infarcted region of the myocardium contributes to preserving diastolic function.

Yontar *et al*. (2021) revealed that MI patients with a higher selvester score had a significantly lower EF, greater troponin levels, a higher injury of the left anterior descending artery, and more adverse events.

Enein *et al*. (2020) evaluated the correlation between the infarct size by MRI and LVEF in a patient with ischemic cardiomyopathy, and they revealed that the scar percentage was higher in patients with a severe decrease in EF, and the scar score was observed as an independent predictor of LVEF improvement after management.

5.5. Receiver operating characteristic sensitivity and specificity for LV remodelling indices:

5.5.1. The cutoff value for 3D-sphericity index:

In this study, the sensitivity and specificity for 3D-SI were (83%, 82%) of the cutoff value 0.33, which approximates the values of the study done by Yang and Zeng (2015) in patients with LV remodelling in non-acute MI the critical value of 3D-SI was 0.32.

In a study done by Mannaerts and Van Der Heide (2004) involving 33 patients with acute anterior MI, the cutoff value of 3D-SI was above 0.25 with sensitivity, a specificity, and AUC were (100%, 90%, and 0.963), this low cutoff value in this study because MI was acute, and this cutoff can differentiate patients with and without subsequent development of LV remodelling.

Another study showed the cutoff value of the sphericity index by 3DE in AMI patients, one month and six months after MI, was 0.28 with sensitivity, specificity, and AUC (83.3%, 95.5%, and 0.891) respectively (Li *et al*., 2008).

The result of 3D-SI in patients with LV remodelling, 6 months after MI was 0.34, 0.35 (Vieira *et al*., 2013; El-Naggar *et al*., 2023), respectively, but the cutoff value was not evaluated.

These results are in contradiction with a study by Karuzas and his co-workers (2019) that included 75 patients with AMI, 3DE performed within 3 days and 6 months later after MI, the cutoff value of 3D-SI was >0.50, sensitivity was 90%, specificity was 91%, and the AUC was 0.957.

5.5.2. The cutoff value for 2D-sphericity index:

For this study, the area under the curve (AUC) for 2D-SI was 0.75, with a sensitivity of 74% and a specificity of 70% for a cutoff value of 0.53.

The results of 2D-SI in other studies were 0.53 in patients with ischemic anterior cardiomyopathy, 0.56 in patients with anterior remodelling after MI, and 0.62 in patients with ischemic cardiomyopathy (Di Donato *et al*., 2006; Garatti *et al*., 2015; Ohira *et al*., 2018) respectively, but the cutoff value was not evaluated in the studies above.

5.5.3.The cutoff value for conicity index:

For this study, the area under the curve (AUC) for CI was 0.78, with sensitivity of 71% and specificity of 74% for a cutoff value of 0.62**.**

Up to our knowledge, no previous study assessed the CI cutoff value, but the results of the conicity index in some studies were 0.76 in patients with anterior MI, 0.88 in patients with anterior remodelling after MI, and 0.73 in patients with ischemic cardiomyopathy (Di Donato *et al*., 2006; Garatti *et al*., 2015; Ohira *et al*., 2018) respectively.

Conclusion and Recommendation

Conclusions

1. This study showed that 2D and 3D-SI are straightforward noninvasive measures of LV remodelling, and, from the correlation studies, can reflect the systolic and diastolic functions of the LV.

2. 3D-SI might be superior because of its higher specificity and sensitivity in comparison with other indices, and the close proximity of values between 3D-SI and SIv measured by equation may give a hint that it could be of benefit in the absence of 3D modality.

3. The conicity index can reflect the regional changes in apical shape produced by anterior infarction.

4. The selvester QRS score was feasible for detecting myocardial scarring in patients with anterior myocardial infarction and can reflects the left ventricular remodelling through its relationship with 2D and 3D-SI, but cannot reflect the regional changes represented by CI.

5. The degree of MR was affected by the raising in SI, while the CI had no effect on MR severity.

6. Clear differences were found between 2D and 3D echocardiographic parameters, which highlights the importance of depending on the 3D echo modality in assessing the severity of LV dysfunction in MI.

Recommendations

1. 3D echocardiographic parameters like EF, SI, and 2D-CI are better to be involved in the assessment of patients with anterior MI for the detection of the severity of the condition and for subsequent follow up.

2. Estimate the LV infarct size from the QRS score to reflect the level of LV scarring and the severity of the condition.

3. To further continue this study on patients with MI with a larger sample size and study the prognostic effect of sphericity and conicity index ratio on the fate of patients in accordance with the severity of the ratio.

4. Assessment of CI in patients with DCM (ischemic and non ischemic) to predict its role in the differentiation of the two conditions.

5. Make a prospective study of patients with acute MI and measure the changes in LV remodelling indices and the prognostic cutoff value.

6. Studying the response to treatment (either medical or interventional therapy) and rate improvement in accordance with changes in remodelling indices.

Reference

Reference

Adhyapak S. M., Thomas T., Jose M. T. & Varghese K. (2022). Effect of left ventricular geometric remodeling on restrictive filling pattern and survival in ischemic cardiomyopathy. Indian Heart Journal, 74(3), 206-211.

Aggarwal A., Srivastava S. & Velmurugan M. (2016). Newer perspectives of coronary artery disease in young. World Journal of Cardiology, 8(12), 728.

Al-Asadi J. N. & Kadhim F. N. (2014). Day of admission and risk of myocardial infarction mortality in a cardiac care unit in Basrah, Iraq. Nigerian Journal of Clinical Practice, 17(5), 579-584.

Albrektsen G., Heuch I., Løchen M. L., Thelle D. S., Wilsgaard T., Njølstad I. & Bønaa K. H. (2016). Lifelong gender gap in risk of incident myocardial infarction: the Tromsø study. JAMA internal medicine, 176(11), 1673-1679.

Amen S. O., Baban S. T., Yousif S. H., Hawez A. H., Baban Z. T. & Jalal D. M. (2020). Prevalence of the most frequent risk factors in Iraqi patients with acute myocardial infarction. Med J Babylon, 17(1), 6-18.

Anderson J. L. & Morrow D. A. (2017). Acute myocardial infarction. New England Journal of Medicine, 376(21), 2053-2064.

Andersson C. & Vasan R. S. (2018). Epidemiology of cardiovascular disease in young individuals. Nature Reviews Cardiology, 15(4), 230-240.

Anvari S., Akbarzadeh M. A., Bayat F., Namazi M. H. & Safi M. (2018). Left ventricular sphericity index analysis for the prediction of appropriate implantable cardioverter-defibrillator therapy. Pacing and Clinical Electrophysiology, 41(9), 1192-1196.

Arısoy F., Ozcan Celebi O., Erbay İ., Tufekcioglu O., Aydoğdu S. & Temizhan A. (2021). Selvester score predicts implantable cardioverter defibrillator shocks in patients with non-ischemic cardiomyopathy. Journal of Arrhythmia, 37(4), 1046-1051.

Armstrong W. F. & Ryan T. (2019). Feigenbaums echocardiography, eight edition. Wolters Kluwer, Philadelphia.

Avila-Vanzzini N., Michelena H. I., Fritche Salazar J. F., Herrera-Bello H., Siu Moguel S., Rodriguez Ocampo R. R. & Espinola Zavaleta N. (2018). Clinical and echocardiographic factors associated with mitral plasticity in patients with chronic inferior myocardial infarction. European Heart Journal-Cardiovascular Imaging, 19(5), 508-515.

Azevedo P. S., Polegato B. F., Minicucci M. F., Paiva S. A. & Zornoff L. A. (2015). Cardiac remodeling: concepts, clinical impact, pathophysiological mechanisms and pharmacologic treatment. Arquivos brasileiros de cardiologia, 106(1), 62-69.

Badano L. P. (2014). The clinical benefits of adding a third dimension to assess the left ventricle with echocardiography. Scientifica, 2014.

Baldea S. M., Velcea A. E., Rimbas R. C., Andronic A., Matei L., Calin S. I. & Vinereanu D. (2021). 3-D echocardiography is feasible and more reproducible than 2-D echocardiography for in-training echocardiographers in follow-up of patients with heart failure

with reduced ejection fraction. Ultrasound in Medicine & Biology, 47(3), 499-510.

Baliga R. R. & Abraham W. T. (2018). Color atlas and synopsis of heart failure. McGraw Hill, New York.

Behairy N. H. E. D., Homos M., Ramadan A., & Gouda S. O. E. S. (2014). Evaluation of left ventricle diastolic dysfunction in ischemic heart disease by CMR: Correlation with echocardiography and myocardial scarring. The Egyptian Journal of Radiology and Nuclear Medicine, 45(4), 1099-1104.

Benjamin E. J., Muntner P., Alonso A., Bittencourt M. S., Callaway C. W., Carson A. P & American Heart Association Council on Epidemiology and Prevention Statistics Committee and Stroke Statistics Subcommittee. (2019). Heart disease and stroke statistics—2019 update: a report from the American Heart Association. Circulation, 139(10), e56-e528.

Bhatt A. S., Ambrosy A. P. & Velazquez E. J. (2017). Adverse remodeling and reverse remodeling after myocardial infarction. Current cardiology reports, 19(8), 1-10.

Biering-Sørensen T., Jensen J. S., Pedersen S., Galatius S., Hoffmann S., Jensen M. T. & Mogelvang R. (2014). Doppler tissue imaging is an independent predictor of outcome in patients with ST-segment elevation myocardial infarction treated with primary percutaneous coronary intervention. Journal of the American Society of Echocardiography, 27(3), 258-267.

Boulet J. & Mehra M. R. (2021). Left Ventricular Reverse Remodeling in Heart Failure: Remission to Recovery. Structural Heart, 5(5), 466-481.

Caballero B. (2019). Humans against obesity: who will win?. Advances in nutrition, 10(1), S4-S9.

Chew D. S., Wilton S. B., Kavanagh K., Southern D. A., Tan-Mesiatowsky L. E. & Exner D. V. (2018). Left ventricular ejection fraction reassessment post–myocardial infarction: Current clinical practice and determinants of adverse remodeling. American heart journal, 198, 91-96.

Choi J. O., Daly R. C., Lin G., Lahr B. D., Wiste H. J., Beaver T. M. & Oh J. K. (2015). Impact of surgical ventricular reconstruction on sphericity index in patients with ischaemic cardiomyopathy: follow-up from the STICH trial. European journal of heart failure, 17(4), 453-463.

Christensen D. M., Strange J. E., Phelps M., Schjerning A. M., Sehested T. S., Gerds T. & Gislason G. (2022). Age-and sex-specific trends in the incidence of myocardial infarction in Denmark, 2005 to 2021. Atherosclerosis, 346(2022), 63-67.

Chumarnaya T. V., Alueva Y. S., Kochmasheva V. V., Mihailov S. P., Revishvili A. S., Tsyv'ian P. B. & Solov'eva O. E. (2016). Features of the left ventricular functional geometry in patients with myocardial diseases with varying degrees of systolic dysfunction. Bulletin of experimental biology and medicine, 162(1), 30-34.

Chung H., Yoon J. H., Yoon Y. W., Park C. H., Ko E. J., Kim,J. Y. & Choi E. Y. (2014). Different contribution of extent of myocardial injury to left ventricular systolic and diastolic function in early reperfused acute myocardial infarction. Cardiovascular Ultrasound, 12(6), 1-10.

Ciftci O., Yilmaz K. C., Karacaglar E., Akgun A. N., Yilmaz M., Oguz A. & Muderrisoglu I. H. (2019). The role of selvester score on 12-lead ECG in determination of left ventricular systolic dysfunction among patients receiving trastuzumab therapy. Uropean journal of therapeutics, 25(1), 69-75.

Coutinho T. (2014). Arterial stiffness and its clinical implications in women. Canadian Journal of Cardiology, 30(7), 756-764.

Curley D., Lavin Plaza B., Shah A. M. & Botnar R. M. (2018). Molecular imaging of cardiac remodelling after myocardial infarction. Basic research in cardiology, 113(2), 1-18.

Dawood H. A. (2015). Assessment of Myocardial Infarction Risk among Patients in Babylon City. Al-Qadisiyah Medical Journal, 11(20), 227-238.

Di Donato M., Dabic P., Castelvecchio S., Santambrogio C., Brankovic J., Collarini L. & Restore Group. (2006). Left ventricular geometry in normal and post-anterior myocardial infarction patients: sphericity index and ‘new’conicity index comparisons. European journal of cardio-thoracic surgery, 29(1), S225-S230.

Dogan C., Omaygenc O., Hatipoglu S., Bakal R. B., Demirkiran A., Emiroglu M. Y. & Ozdemir N. (2013). Assessment of ST-Elevation Myocardial Infarction–Related Diastolic Dysfunction

with Compensatory Rise in Left Atrial Ejection Force. Echocardiography, 30(3), 279-284.

Duraes A. R., Bitar Y. S., Freitas A. C. T., Ivan Filho M. P., Freitas B. C. & Fernandez A. M. (2017). Gender differences in ST-elevation myocardial infarction (STEMI) time delays: experience of a public health service in Salvador-Brazil. American Journal of Cardiovascular Disease, 7(5), 102.

Elden A. (2015). Post Myocardial Infarction Remodelling. Journal of medical science and clinical research, 3(12), 8735-8744.

El-Naggar H. M., Osman A. S., Ahmed M. A., Youssef A. A. & Ahmed T. A. (2023). Three-dimensional echocardiographic assessment of left ventricular geometric changes following acute myocardial infarction. The International Journal of Cardiovascular Imaging, 39(3), 607-620.

Emara A. A., Hafez A. O., Abdo Eldeeb H. M. (2021). Relation of sphericity index to left ventricular twist in patients with ischemic cardiomyopathy, speckle tracking study. Journal of cardiovascular disease research, 12(1), 146–150.

Enein F. A., Allaaboun S., Khayyat S., Andijani M., Alkhuzai M. M., Aljunied A. A. & Al Adhreai Sr M. (2020). Association Between Myocardial Scar Burden and Left Ventricular Ejection Fraction in Ischemic Cardiomyopathy. Cureus, 12(12), e12110.

Fan H., Zheng Z., Feng W., Zhang Y., Jin L., Li P. & Hu S. (2010). Apical conicity ratio: a new index on left ventricular apical geometry after myocardial infarction. The Journal of thoracic and cardiovascular surgery, 140(6), 1402-1407.

Ferrante G., Barbieri L., Sponzilli C., Lucreziotti S., Salerno Uriarte D., Centola M. & Carugo S. (2021). Predictors of mortality and long-term outcome in patients with anterior stemi: Results from a single center study. Journal of Clinical Medicine, 10(23), 5634.

Flachskampf F. A. (2010). Raised diastolic pressure as an early predictor of left ventricular remodeling after infarction: should echocardiography or natriuretic peptides be used for assessment?. Revista Española de Cardiología, 63(9), 1009-1012.

Frantz S., Hundertmark M. J., Schulz-Menger J., Bengel F. M. & Bauersachs J. (2022). Left ventricular remodelling post-myocardial infarction: pathophysiology, imaging, and novel therapies. European Heart Journal, 43(27), 2549-2561.

Fukuda S., Watanabe H., Daimon M., Abe Y., Hirashiki A., Hirata K. & Yoshikawa J. (2012). Normal Values of Real-Time 3-Dimensional Echocardiographic Parameters in a Healthy Japanese Population–The JAMP-3D Study–. Circulation Journal, 76(5), 1177-1181.

Galderisi M., Cosyns B., Edvardsen T., Cardim N., Delgado V., Di Salvo G. &Habib G. (2017). Standardization of adult transthoracic echocardiography reporting in agreement with recent chamber quantification, diastolic function, and heart valve disease recommendations: an expert consensus document of the European Association of Cardiovascular Imaging. European Heart Journal-Cardiovascular Imaging, 18(12), 1301-1310.

Garatti A., Castelvecchio S., Bandera F., Guazzi M. & Menicanti L. (2015). Surgical ventricular restoration: is there any difference in

outcome between anterior and posterior remodeling?. The Annals of Thoracic Surgery, 99(2), 552-559.

Garza M. A., Wason E. A. & Zhang J. Q. (2015). Cardiac remodeling and physical training post myocardial infarction. World journal of cardiology, 7(2), 52.

Ghadri J. R., Wittstein I. S., Prasad A., Sharkey S., Dote, K., Akashi Y. J. & Templin C. (2018). International expert consensus document on Takotsubo syndrome (part II): diagnostic workup, outcome, and management. European Heart Journal, 39(22), 2047-2062.

Guo H., Zhou X., Xu J., Ye Z., Guo L. & Huang R. (2022). QRS score: A simple marker to quantify the extent of myocardial scarring in patients with chronic total arterial occlusion. Chronic Diseases and Translational Medicine, 8(1), 51-58.

Halima A. B. & Zidi A. (2018). The cardiac magnetic resonance sphericity index in the dilated cardiomyopathy: new diagnostic and prognostic marker. Archives of Cardiovascular Diseases Supplements, 10(1), 42.

Harris S., Hamed A., Ali M. M. & Hussien A. (2019). Determinant factors of noncompliance on treatment among hypertensive patients attending outpatient clinic in sohag university hospital. Sohag Medical Journal, 23(3), 105-110.

Herrett E., Gallagher A. M., Bhaskaran K., Forbes H., Mathur R., Van Staa T., & Smeeth L. (2015). Data resource profile: clinical practice research datalink (CPRD). International journal of epidemiology, 44(3), 827-836.

Heusch G. & Gersh B. J. (2017). The pathophysiology of acute myocardial infarction and strategies of protection beyond reperfusion: a continual challenge. European heart journal, 38(11), 774-784.

Holmes L. E., Nguyen T. L., Hee L., Otton J., Moses D. A., French J. K. & Juergens C. P. (2016). Electrocardiographic measurement of infarct size compared to cardiac MRI in reperfused first time ST-segment elevation myocardial infarction. International Journal of Cardiology, 220(2016), 389-394.

Ioacara S., Popescu A. C., Tenenbaum J., Dimulescu D. R., Popescu M. R., Sirbu A., & Fica S. (2020). Acute myocardial infarction mortality rates and trends in Romania between 1994 and 2017. International Journal of Environmental Research and Public Health, 17(1), 285.

Jan M. F. & Tajik A. J. (2017). Modern imaging techniques in cardiomyopathies. Circulation research, 121(7), 874-891.

Kalogeropoulos A. P., Georgiopoulou V. V., Gheorghiade M. & Butler J. (2012). Echocardiographic evaluation of left ventricular structure and function: new modalities and potential applications in clinical trials. Journal of cardiac failure, 18(2), 159-172.

Kaolawanich Y. & Boonyasirinant T. (2019). Usefulness of apical area index to predict left ventricular thrombus in patients with systolic dysfunction: a novel index from cardiac magnetic resonance. BMC cardiovascular disorders, 19(1), 1-8.

Kaplangoray M., Aydın C., Toprak K. & Cekici Y. (2023). Selvester score and myocardial performance index in acute anterior

myocardial infarction. Revista da Associação Médica Brasileira, 69(2), 325-329.

Karakuş A., & Berat U. Ğ. U. Z. (2020). Prognostic value of the Selvester QRS score for re-hospitalization in patients with ischemic heart failure. Journal of Surgery and Medicine, 4(12), 1165-1168.

Karuzas A., Rumbinaite E., Verikas D., Ptasinskas T., Muckiene G., Kazakauskaite E., Zabiela V., Jurkevicius R., Vaskelyte JJ., Zaliunas R., & Zaliaduonyte-Peksiene D. (2019). Accuracy of three-dimensional systolic dyssynchrony and sphericity indexes for identifying early left ventricular remodeling after acute myocardial infarction. Anatolian Journal of Cardiology, 22(1), 13.

Khanna S., Bhat A., Chen H. H., Tan J. W., Gan G. C. & Tan T. C. (2020). Left Ventricular Sphericity Index is a reproducible bedside echocardiographic measure of geometric change between acute phase Takotsubo's syndrome and acute anterior myocardial infarction. IJC Heart & Vasculature, 29(2020), 100547.

Khanna S., Tan J., Chen H., Bhat A., Gan G. & Tan T. (2020). Left Ventricular Sphericity Index is a Predictor of Cardiovascular Events in Patients With Anterior Transmural Myocardial Infarction but not in Takotsubo Syndrome. Heart, Lung and Circulation, 29(2), S204.

Kossaify A. & Nasr M. (2019). Diastolic dysfunction and the new recommendations for echocardiographic assessment of left ventricular diastolic function: Summary of guidelines and

novelties in diagnosis and grading. Journal of Diagnostic Medical Sonography, 35(4), 317-325.

Lancellotti P., Zamorano J. L., Habib G., Badano L. (2017). The EACVI textbook of echocardiography, second edition. Oxford University Press, United Kingdom.

Lancellotti P., Price S., Edvardsen T., Cosyns B., Neskovic A. N., Dulgheru R. & Habib G. (2015). The use of echocardiography in acute cardiovascular care: recommendations of the European Association of Cardiovascular Imaging and the Acute Cardiovascular Care Association. European Heart Journal-Cardiovascular Imaging, 16(2), 119-146.

Lang R. M., Badano L. P., Mor-Avi V., Afilalo J., Armstrong A., Ernande L. & Voigt J. U. (2015). Recommendations for cardiac chamber quantification by echocardiography in adults: an update from the American Society of Echocardiography and the European Association of Cardiovascular Imaging. European Heart Journal-Cardiovascular Imaging, 16(3), 233-271.

Lang R. M., Badano L. P., Tsang W., Adams D. H., Agricola E., Buck T. & Zoghbi W. A. (2012). EAE/ASE recommendations for image acquisition and display using three-dimensional echocardiography. European Heart Journal–Cardiovascular Imaging, 13(1), 1-46.

Le H. T., Hangiandreou N., Timmerman R., Rice M. J., Smith W. B., Deitte L. & Janelle G. M. (2016). Imaging artifacts in echocardiography. Anesthesia & Analgesia, 122(3), 633-646.

Leancă S. A., Crișu D., Petriș A. O., Afrăsânie I., Genes A., Costache A. D. & Costache I. I. (2022). Left ventricular remodeling after myocardial infarction: From physiopathology to treatment. Life, 12(8), 1111.

Li F., Chen Y. G., Yao G. H., Li L., Ge Z. M., Zhang M. & Zhang Y. (2008). Usefulness of left ventricular conic index measured by real-time three-dimensional echocardiography to predict left ventricular remodeling after acute myocardial infarction. The American journal of cardiology, 102(11), 1433-1437.

Liu Q., Zhang Y., Zhang P., Zhang J., Cao X., He S. & Yang D. (2020). Both baseline Selvester QRS score and change in QRS score predict prognosis in patients with acute ST-segment elevation myocardial infarction after percutaneous coronary intervention. Coronary Artery Disease, 31(5), 403.

Loring Z., Chelliah S., Selvester R. H., Wagner G. & Strauss D. G. (2011). A detailed guide for quantification of myocardial scar with the Selvester QRS score in the presence of electrocardiogram confounders. Journal of electrocardiology, 44(5), 544-554.

Maffessanti F., Gripari P., Addetia K., Tamborini G., Muratori M., Weinert L. & Lang R. (2014). Relationship between mitral regurgitation and left ventricular remodeling: importance of 3d echocardiographic assessment of ventricular shape in dilated cardiomyopathy. Journal of the American College of Cardiology, 63(12S), A1168-A1168.

Maffessanti F., Lang R. M., Corsi C., Mor-Avi V. & Caiani E. G. (2009). Feasibility of left ventricular shape analysis from transthoracic real-time 3-D echocardiographic images. Ultrasound in medicine & biology, 35(12), 1953-1962.

Mannaerts H. F., van der Heide J. A., Kamp O., Stoel M. G., Twisk J. & Visser C. A. (2004). Early identification of left ventricular remodelling after myocardial infarction, assessed by transthoracic 3D echocardiography. European heart journal, 25(8), 680-687.

Markendorf S., Benz D. C., Messerli M., Grossmann M., Giannopoulos A. A., Patriki D. & Gaemperli O. (2021). Value of 12-lead electrocardiogram to predict myocardial scar on FDG PET in heart failure patients. Journal of Nuclear Cardiology, 28(4), 1364-1373.

Masci P. G., Ganame J., Francone M., Desmet W., Lorenzoni V., Iacucci I. & Bogaert J. (2011). Relationship between location and size of myocardial infarction and their reciprocal influences on post-infarction left ventricular remodelling. European heart journal, 32(13), 1640-1648.

Matsumura Y., Gillinov A. M., Toyono M., Oe H., Yamano T., Takasaki K., Saraiva R. M. & Shiota T. (2010). Echocardiographic predictors for persistent functional mitral regurgitation after aortic valve replacement in patients with aortic valve stenosis. The American journal of cardiology, 106(5), 701-706.

Mitchell C., Rahko P. S., Blauwet L. A., Canaday B., Finstuen J. A., Foster M. C., Horton K., Ogunyankin K. O., Palma R. A. & Velazquez E. J. (2019). Guidelines for performing a

comprehensive transthoracic echocardiographic examination in adults: recommendations from the American Society of Echocardiography. Journal of the American Society of Echocardiography, 32(1), 1-64.

Mitter S. S., Shah S. J. & Thomas J. D. (2017). A test in context: E/A and E/e′ to assess diastolic dysfunction and LV filling pressure. Journal of the American College of Cardiology, 69(11), 1451-1464.

Mohseni J., Kazemi T., Maleki M. H. & Beydokhti H. (2017). A systematic review on the prevalence of acute myocardial infarction in Iran. Heart views: the official journal of the Gulf Heart Association, 18(4), 125.

Moore C. R., Jain S., Haas S., Yadav H., Whitsel E., Rosamand W. & Kucharska-Newton A. M. (2021). Ascertaining Framingham heart failure phenotype from inpatient electronic health record data using natural language processing: a multicentre Atherosclerosis Risk in Communities (ARIC) validation study. BMJ open, 11(6), e047356.

Muraru D., Badano L. P., Peluso D., Dal Bianco L., Casablanca S., Kocabay G., Zoppellaro G. & Iliceto S. (2013). Comprehensive analysis of left ventricular geometry and function by three-dimensional echocardiography in healthy adults. Journal of the American Society of Echocardiography, 26(6), 618-628.

Myhr K. A., Pedersen F. H., Kristensen C. B., Visby L., Hassager C. & Mogelvang R. (2018). Semi-automated estimation of left ventricular ejection fraction by two-dimensional and three-

dimensional echocardiography is feasible, time-efficient, and reproducible. Echocardiography, 35(11), 1795-1805.

Nagueh S. F., Smiseth O. A., Appleton C. P., Byrd B. F., Dokainish H., Edvardsen T. & Texas H. (2016). Recommendations for the evaluation of left ventricular diastolic function by echocardiography: an update from the American Society of Echocardiography and the European Association of Cardiovascular Imaging. European Journal of Echocardiography, 17(12), 1321-1360.

Nakamori S., Ismail H., Ngo L. H., Manning W. J. & Nezafat R. (2017). Left ventricular geometry predicts ventricular tachyarrhythmia in patients with left ventricular systolic dysfunction: a comprehensive cardiovascular magnetic resonance study. Journal of Cardiovascular Magnetic Resonance, 19(1), 1-10.

Nappi F., Spadaccio C., Chello M. & Mihos C. G. (2017). Papillary muscle approximation in mitral valve repair for secondary MR. Journal of Thoracic Disease, 9(7), S635 -S639.

Nishimura R. A., Otto C. M., Bonow R. O., Carabello B. A., Erwin J. P., Guyton R. A. & Thomas J. D. (2014). 2014 AHA/ACC guideline for the management of patients with valvular heart disease: a report of the American College of Cardiology/American Heart Association Task Force on Practice Guidelines. Circulation, 129(23), e521-e643.

Nishino S., Watanabe N., Kimura T., Enriquez-Sarano M., Nakama T., Furugen M. & Shibata Y. (2016). The course of ischemic mitral regurgitation in acute myocardial infarction after primary

percutaneous coronary intervention: from emergency room to long-term follow-up. Circulation: Cardiovascular Imaging, 9(8), e004841.

Nowbar A. N., Gitto M., Howard J. P., Francis D. P. & Al-Lamee, R. (2019). Mortality from ischemic heart disease: Analysis of data from the World Health Organization and coronary artery disease risk factors From NCD Risk Factor Collaboration. Circulation: cardiovascular quality and outcomes, 12(6), e005375.

Oh J. K., Velazquez E. J., Menicanti L., Pohost G. M., Bonow R. O., Lin G. & STICH Investigators. (2013). Influence of baseline left ventricular function on the clinical outcome of surgical ventricular reconstruction in patients with ischaemic cardiomyopathy. European heart journal, 34(1), 39-47.

Ohira S., Yamazaki S., Numata S., Kawajiri H., Morimto K., Doi K. & Yaku H. (2018). Ten-year experience of endocardial linear infarct exclusion technique for ischaemic cardiomyopathy. European Journal of Cardio-Thoracic Surgery, 53(2), 440-447.

Oktay A. A., Rich J. D. & Shah S. J. (2013). The emerging epidemic of heart failure with preserved ejection fraction. Current heart failure reports, 10(4), 401-410.

Ola R. K., Meena C. B., Ramakrishnan S., Agarwal A. & Bhargava S. (2018). Detection of left ventricular remodeling in acute ST elevation myocardial infarction after primary percutaneous coronary intervention by two dimensional and three dimensional echocardiography. Journal of Cardiovascular Echography, 28(1), 39-44.

Ørn S., Manhenke C., Anand I. S., Squire I., Nagel E., Edvardsen T. & Dickstein K. (2007). Effect of left ventricular scar size, location, and transmurality on left ventricular remodeling with healed myocardial infarction. The American journal of cardiology, *99*(8), 1109-1114.

Osadchii O. E., Norton G. R., McKechnie R., Deftereos D. & Woodiwiss A. J. (2007). Cardiac dilatation and pump dysfunction without intrinsic myocardial systolic failure following chronic β-adrenoreceptor activation. American Journal of Physiology-Heart and Circulatory Physiology, 292(4), H1898-H1905.

Padala S. K., Cabrera J. A. & Ellenbogen K. A. (2021). Anatomy of the cardiac conduction system. Pacing and Clinical Electrophysiology, 44(1), 15-25.

Palmiero P., Zito A., Maiello M., Cameli M., Modesti P. A., Muiesan M. L. & Ciccone M. M. (2015). Left ventricular diastolic function in hypertension: methodological considerations and clinical implications. Journal of clinical medicine research, 7(3), 137-144.

Papolos A., Narula J., Bavishi C., Chaudhry F. A. & Sengupta P. P. (2016). US hospital use of echocardiography: insights from the nationwide inpatient sample. Journal of the American College of Cardiology, 67(5), 502-511.

Pezel T., Des Horts T. B., Schaaf M., Croisille P., Bière L., Garcia-Dorado D. & Mewton N. (2020). Predictive value of early cardiac magnetic resonance imaging functional and geometric indexes for adverse left ventricular remodelling in patients with

anterior ST-segment elevation myocardial infarction: A report from the CIRCUS study. Archives of cardiovascular diseases, 113(11), 710-720.

Ponikowski P., Voors A. A., Anker S. D., Bueno H., Cleland J. G., Coats A. J. & van der Meer, P. E. S. C. (2016). ESC Scientific Document Group. 2016 ESC Guidelines for the diagnosis and treatment of acute and chronic heart failure: The Task Force for the diagnosis and treatment of acute and chronic heart failure of the European Society of Cardiology (ESC) Developed with the special contribution of the Heart Failure Association (HFA) of the ESC. *Eur Heart J*, 37(27), 2129-2200.

Poon J., Leung J. T. & Leung D. Y. (2019). 3D echo in routine clinical practice–state of the art in 2019. Heart, Lung and Circulation, 28(9), 1400-1410.

Popović Z. B., Desai M. Y., Buakhamsri A., Puntawagkoon C., Borowski A., Levine B. D. & Thomas J. D. (2011). Predictors of mitral annulus early diastolic velocity: impact of long-axis function, ventricular filling pattern, and relaxation. European Journal of Echocardiography, 12(11), 818-825.

Prasad S. B., Lin A. K., Guppy-Coles K. B., Stanton T., Krishnasamy R., Whalley G. A. & Atherton J. J. (2018). Diastolic dysfunction assessed using contemporary guidelines and prognosis following myocardial infarction. Journal of the American Society of Echocardiography, 31(10), 1127-1136.

Price D. (2010). How to read an electrocardiogram (ECG). Part 1: Basic principles of the ECG. The normal ECG. South Sudan Medical Journal, 3(2), 26-31.

Rathore V., Singh N., Mahat R. K., Kocak M. Z., Fidan K., Ayazoglu T. A. & Yolcu A. (2018). Risk factors for acute myocardial infarction: a review. *EJMI*, 2(1), 1-7.

Reindl M., Reinstadler S. J., Tiller C., Feistritzer H. J., Kofler M., Brix A. & Metzler B. (2019). Prognosis-based definition of left ventricular remodeling after ST-elevation myocardial infarction. European Radiology, 29(5), 2330-2339.

Rigolli M., Anandabaskaran S., Christiansen J. P. & Whalley G. A. (2016). Bias associated with left ventricular quantification by multimodality imaging: a systematic review and meta-analysis. Open Heart, 3(1), e000388.

Rodríguez-Zanella H., Muraru D., Secco E., Boccalini F., Azzolina D., Aruta P. & Badano L. P. (2019). Added value of 3-versus 2-dimensional echocardiography left ventricular ejection fraction to predict arrhythmic risk in patients with left ventricular dysfunction. JACC: Cardiovascular Imaging, 12(10), 1917-1926.

Rørholm Pedersen L., Frestad D., Mide Michelsen M., Dam Mygind N., Rasmusen H., Elena Suhrs H. & Prescott E. (2016). Risk factors for myocardial infarction in women and men: a review of the current literature. Current pharmaceutical design, 22(25), 3835-3852.

Rosengarten J. A., Scott P. A., Chiu O. K., Shambrook J. S., Curzen N. P. & Morgan J. M. (2013). Can QRS scoring predict left ventricular scar and clinical outcomes?. Europace, 15(7), 1034-1041.

Roth G. A., Johnson C., Abajobir A., Abd-Allah F., Abera S. F., Abyu G. & Ukwaja K. N. (2017). Global, regional, and national burden of cardiovascular diseases for 10 causes, 1990 to 2015. Journal of the American college of cardiology, 70(1), 1-25.

Rovers W. C., van Boreen M. C., Robinson M., Martin T. N., Maynard C., Wagner G. S. & Gorgels A. P. (2009). Comparison of the correlation of the Selvester QRS scoring system with cardiac contrast-enhanced magnetic resonance imaging–measured acute myocardial infarct size in patients with and without thrombolytic therapy. Journal of Electrocardiology, 42(2), 139-144.

Sadeghpour A., Abtahi F., Kiavar M., Esmaeilzadeh M., Samiei N., Ojaghi S. Z. & Mohebbi A. (2008). Echocardiographic evaluation of mitral geometry in functional mitral regurgitation. Journal of cardiothoracic surgery, 3(1), 1-7.

Saleh M. & Ambrose J. A. (2018). Understanding myocardial infarction. F1000Research, 7.

Sharif B. O. & Lafi S. Y. (2021). Common Risk Factors of Myocardial Infarction and Some Socio Demographic Characteristics in Sulaimani City. Kurdistan Journal of Applied Research,6(2), 136-143.

Silveira C. F. D. S. M. P. D., Malagutte K. N. D. S., Nogueira B. F., Reis F. M., Rodrigues C. D. S. A., Rossi D. A. A. & Bazan S. G. Z. (2021). Clinical and echocardiographic predictors of left

ventricular remodeling following anterior acute myocardial infarction. Clinics, 76, e2732.

Simpson J. M. & Miller O. (2011). Three-dimensional echocardiography in congenital heart disease. Archives of cardiovascular diseases, 104(1), 45-56.

Søholm H., Lønborg J., Andersen M. J., Vejlstrup N., Engstrøm T., Hassager C. & Møller J. E. (2016). Association diastolic function by echo and infarct size by magnetic resonance imaging after STEMI. Scandinavian Cardiovascular Journal, 50(3), 172-179.

Strauss D. G. & Selvester R. H. (2009). The QRS complex-a biomarker that" images" the heart: QRS scores to quantify myocardial scar in the presence of normal and abnormal ventricular conduction. Journal of electrocardiology, 42(1), 85.

Strauss D. G., Selvester R. H., Lima J. A., Arheden H., Miller J. M., Gerstenblith G. & Wu K. C. (2008). ECG quantification of myocardial scar in cardiomyopathy patients with or without conduction defects: correlation with cardiac magnetic resonance and arrhythmogenesis. Circulation: Arrhythmia and Electrophysiology, 1(5), 327-336.

Sundqvist M. G., Verouhis D., Sorensson P., Henareh L., Persson J., Saleh N. & Ugander M. (2022). The size of myocardial infarction and peri-infarction edema are not major determinants of diastolic impairment after acute myocardial infarction. medRxiv, 2022, 07.

Tanabe K. (2020). Three-dimensional echocardiography role in clinical practice and future directions. Circulation journal,84(7), 1047-1054.

Tani L. Y., Minich L. L., Williams R. V. & Shaddy R. E. (2005). Ventricular remodeling in children with left ventricular dysfunction secondary to various cardiomyopathies. The American journal of cardiology, 96(8), 1157-1161.

Thygesen K., Alpert J. S., Jaffe A. S., Chaitman B. R., Bax J. J., Morrow D. A., White H. D. & Fox K. A. A. (2018). Fourth universal definition of myocardial infarction. Circulation, 138(20), e618-e651.

Tiller C., Reindl M., Reinstadler S. J., Holzknecht M., Schreinlechner M., Peherstorfer A. & Metzler B. (2019). Complete versus simplified Selvester QRS score for infarct severity assessment in ST-elevation myocardial infarction. BMC Cardiovascular Disorders, 19(1), 1-7.

Tjandrawidjaja M. C., Fu Y., Westerhout C. M., Wagner G. S., Granger C. B., Armstrong P. W. & APEX-AMI Investigators. (2010). Usefulness of the QRS score as a strong prognostic marker in patients discharged after undergoing primary percutaneous coronary intervention for ST-segment elevation myocardial infarction. The American journal of cardiology, 106(5), 630-634.

Traina M. I., Almahmeed W., Edris A. & Murat Tuzcu E. (2017). Coronary heart disease in the Middle East and North Africa: current status and future goals. Current atherosclerosis reports, 19(5), 1-6.

van der Bijl P., Abou R., Goedemans L., Gersh B. J., Holmes Jr D. R., Ajmone Marsan N. & Bax J. J. (2020). Left ventricular post-infarct remodeling: implications for systolic function

improvement and outcomes in the modern era. Heart Failure, 8(2), 131-140.

van Eif V. W., Devalla H. D., Boink G. J. & Christoffels V. M. (2018). Transcriptional regulation of the cardiac conduction system. Nature Reviews Cardiology, 15(10), 617-630.

Vieira M. L. C., Oliveira W. A., Cordovil A., Rodrigues A. C. T., Mônaco C. G., Afonso T. & Morhy S. S. (2013). 3D Echo pilot study of geometric left ventricular changes after acute myocardial infarction. Arquivos brasileiros de cardiologia, 101(1), 43-51.

Watanabe N., Isobe S., Okumura T., Mori H., Yamada T., Nishimura K. & Murohara T. (2016). Relationship between QRS score and microvascular obstruction after acute anterior myocardial infarction. Journal of Cardiology, 67(4), 321-326.

Wolff E. F., He Y., Black D. M., Brinton E. A., Budoff M. J., Cedars M. I. & Taylor H. S. (2013). Self-reported menopausal symptoms, coronary artery calcification, and carotid intima-media thickness in recently menopausal women screened for the Kronos early estrogen prevention study (KEEPS). Fertility and sterility, 99(5), 1385-1391.

Wong S. P., French J. K., Lydon A. M., Manda S. O., Gao W., Ashton N. G. & White H. D. (2004). Relation of left ventricular sphericity to 10-year survival after acute myocardial infarction. The American journal of cardiology, 94(10), 1270-1275.

Xiong M. F., Wu L. F., Chen Y. H., Cao R. R., Deng F. Y., & Lei S. F. (2022). Body Surface Area (BSA) is a Better Osteoporosis Associated Anthropometric Parameter Than Other

Anthropometric Parameters in Elderly Population. Journal of Clinical Densitometry, 25(4), 630-636.

Yang H. & Zeng Z. (2015). The value of three-dimensional spherical index in assessing different type of left ventricular remodeling. Journal of the American College of Cardiology, 66(16S), C256-C256.

Yiu S. F., Enriquez-Sarano M., Tribouilloy C., Seward J. B. & Tajik A. J. (2000). Determinants of the degree of functional mitral regurgitation in patients with systolic left ventricular dysfunction: a quantitative clinical study. Circulation, 102(12), 1400-1406.

Yontar O. C., Erdogan G., Yenercag M., Gul S., Arslan U. & Karagoz A. (2021). Relationship between Selvester ECG Score and Cardiovascular Outcomes in Patients with Non-ST Elevation Myocardial Infarction. Acta Cardiologica Sinica, 37(6), 580.

Youn H. J. & Jung H. O. (2016). The Influence of Apical Aneurysm on Left Ventricular Geometry and Clinical Outcomes: 3-Year Follow-Up Using Echocardiography. Echocardiography, 33(6), 814-820.

Zhang Y., Chan A. K., Yu C. M., Lam W. W., Yip G. W., Fung W. H. & Sanderson J. E. (2005). Left ventricular systolic asynchrony after acute myocardial infarction in patients with narrow QRS complexes. American Heart Journal, 149(3), 497-503.

تمت دراسة العلاقة بين هذه المؤشرات والوظائف الانقباضية والانبساطية للبطين الأيسر. تم حساب نقاط السيلفستر من تخطيط القلب ، وتم فحص العلاقة بين حجم الاحتشاء وعوامل إعادة تشكيل البطين الايسر.

كانت هناك فروق معنوية بين المرضى والاصحاء فيما يتعلق بقيم مؤشرات الكرويه ومؤشر المخروطيه (قيمه P < ٠.٠٥).

أظهر مؤشر الكروية (3D,2D) ارتباط عكسي معنوي مع معدل القذف القلبي (3D,2D)، (قيمه P < ٠.٠٠٠)، وارتباط عكسي معنوي مع حجم النفضة، (قيمه P < ٠.٠٥).

أظهر مؤشر المخروطية علاقة عكسية غير معنوية مع معدل القذف القلبي وحجم النفضة (3D,2D)، (P > ٠.٠٥).

فيما يتعلق بدراسة ارتباط مؤشر المخروطية والكروية مع عوامل القلب الانبساطية، اظهرت علاقة طردية غير معنوية (P > ٠.٠٥) وارتباط طردي معنوي مع مؤشر حجم الاذين الايسر (P< ٠.٠٥).

اظهرت دراسة علاقة حجم احتشاء عضلة القلب مع عوامل إعادة تشكيل البطين الايسر، ارتباط طردي معنوي مع مؤشر الكروية (2D)، وارتباطا طردي غير معنوي مع (3D)، قيمة الP =٠.٣٧٧، ٠.٠٤٤ على التوالي، مع عدم وجود ارتباط مع مؤشر المخروطية (P >٠.٠٥).

نستنتج أن مؤشرات البطين الايسر المحددة بتخطيط صدى القلب هي مقياس مباشر لإعادة تشكيل البطين الايسر إما مناطقيا بواسطة مؤشر المخروطية أو شاملا بواسطة مؤشر الكروية (3D,2D) كما يمكنها أن تعكس الوظيفة الانقباضية والانبساطية للبطين الايسر ، وأيضا كانت نقاط السيلفستر مجدية للكشف عن تندب عضلة القلب في المرضى الذين يعانون من احتشاء عضلة القلب الأمامي ويمكن أن تعكس إعادة تشكيل البطين الأيسر من خلال علاقتها مع مؤشر الكروية (3D,2D)، ولكن لا يمكن أن تعكس التغييرات المناطقية المتمثلة بمؤشر المخروطية

الخلاصة

يحمل احتشاء عضلة القلب الأمامي أسوأ نوع مقارنة مع مواقع الاحتشاء الاخرى ، نظرا للمساحة الأكبر لحجم احتشاء عضلة القلب ، فإنه يؤدي إلى سلسلة من التغييرات الهيكلية التي تغير حجم وشكل البطين الأيسر. يخضع القلب لعملية إعادة تشكيل واسعة لعضلة القلب من خلال تراكم الأنسجة الليفية في كل من عضلة القلب المصابة وغير المصابة بالاحتشاء ، مما يشوه بنية الأنسجة ، ويزيد من تصلب الأنسجة ، ويتسبب بضعف البطين. تم استخدام مؤشر الكروية لقياس شكل البطين الأيسر الشامل ، لكنه فشل في اكتشاف تغيرات الشكل المناطقي التي تحدث في المنطقة القمية ، لذلك تم تحديد مقياس مباشر يسمى مؤشر المخروطية لقياس هذه التغييرات. تم إنشاء تقنية تخطيط كهربية القلب تسمى نقاط سيلفستر لتقدير حجم الاحتشاء بعد احتشاء عضلة القلب ، وتتمتع بميزة كونها ميسورة التكلفة ويمكن الوصول إليها.

تهدف هذه الدراسة إلى تقييم دور مؤشر الكروية في القياس الكمي للتغيرات الهندسية للبطين الأيسر ودراسة علاقته بالعمل الانقباضي والانبساطي للقلب، بجانب دور مؤشر المخروطية في عكس التغيرات المناطقية في البطين الايسر، وأيضا فحص دور نقاط سيلفستر في تحديد حجم الندبة لعضلة القلب في المرضى الذين يعانون من احتشاء عضلة القلب الأمامي وعلاقته بإعادة تشكيل البطين الأيسر.

أجريت هذه الدراسة على ١٠٠ شخص (٥٠ مريضا تم تشخيصهم باحتشاء عضلة القلب الأمامي القديم و ٥٠ شخصا سليما).

أجريت الدراسة في مركز الشهيد المحراب لقسطرة القلب ومدينة المرجان الطبية في مدينة الحلة بمحافظة بابل، خلال الفترة من بداية شهر أيلول ٢٠٢٢ وحتى بداية شهر شباط ٢٠٢٣.

خضع المشاركون لتقييم تخطيط صدى القلب الثنائي والثلاثي الابعاد (3D,2D)، بواسطة تخطيط صدى القلب الثنائي ، تم قياس المحاور الطويلة والقصيرة للبطين الأيسر وحساب نسبتهم على أنها مؤشر الكرويه، كما تم قياس طول المحور القمي للبطين الايسر وتم حساب النسبة بين طول المحور القمي والقصير على أنها مؤشر المخروطية. تم قياس مؤشر الكروية أيضا بتخطيط صدى القلب الثلاثي الابعاد ونسبة الحجم، كنسبة بين حجم نهاية الانبساط وحجم الكرة الافتراضي (٦/١ *π * مكعب المحور الطويل للبطين الايسر).

وزارة التعليم العالي و البحث العلمي
جامعه بابل
كلية الطب
فرع الفسلجة الطبية

تقييم إعادة تشكيل البطين الأيسر في مرضى احتشاء عضلة القلب الأمامي عن طريق مؤشر الكروية مشتق من فحص صدى القلب الثنائي والثلاثي الابعاد وبواسطة تخطيط كهربائية القلب

رسالة

مقدمة الى مجلس كلية الطب/ جامعه بابل

كجزء من متطلبات نيل درجة الماجستير في العلوم/ الفسلجة الطبية

من قبل

فاطمة عدنان شهيد جابر

بكالوريوس طب و جراحة عامة- كليه الطب جامعه بابل

اشراف

الاستاذ المساعد الدكتور
احلام كاظم عبود
دكتوراه فسلجة طبية
جامعة بابل

الاستاذ المساعد الدكتور
شكري فائز ناصر
بورد امراض القلب والداخل القسطاري
جامعة بابل

٢٠٢٣ ميلاديه

١٤٤٤ هجريه